Resonance and Transient Behavior of Extensive Cable Grid

Report on Frequency Domain Assessment and Mitigation of Power System Resonances

KU LEUVEN

Energy Ville

This report forms part of the project "Resonance and transient behavior of extensive cable grid", commissioned by Elia Engineering nv/sa, a member of the Elia Group.

Report editor and project coordination: dr. Willem Leterme
Under supervision of prof. Dirk Van Hertem and prof. Jef Beerten
Contributors: dr. Aleksandra Lekić, Rickard Lundholm, Philippe De Rua, Özgür Can Sakıncı
June, 2020
Please refer to this report as: W. Leterme *et al.*, "Resonance and Transient Behavior of Extensive Cable Grid - Report on Frequency Domain Assessment and Mitigation of Power System Resonances", KU Leuven/EnergyVille, Leuven/Genk, Belgium, Project Report, June 2020

Contents

Executive Summary

This report forms part of the project "Resonance and transient behavior of extensive cable grid" and presents a detailed literature review on (i) modelling aspects, (ii) calculation methodologies and their usage in practical studies, (iii) assessment criteria based on the frequency domain results to identify dangerous situations and (iv) mitigation measures related to grid resonances. A case study is included to illustrate the general use of the calculation methodologies and models for studying frequency shifts.

Increasing the share of cables in the power system in general leads to a shift of power system resonances to lower frequencies, thereby possibly introducing problems associated with two phenomena. First, existing background harmonics may be amplified to unacceptable levels, leading to e.g. power quality problems at lower voltage levels. Second, resonances at low frequencies (100-200 Hz) may lie at the origin of (resonant) temporary overvoltages. These overvoltages were found to prevail especially during switching events in weak systems or in systems with a large amount of cables. An example case study in this document confirms that increasing the amount of cables caused a shift of existing resonances to lower frequencies and an increase of resonance peaks in the frequency region up to 2500 Hz.

The literature and industry practice shows that several mitigation methods exist to deal with resonance problems, but some of these may also introduce increased complexity in planning and operating the grid (e.g. applying filters), or may interfere with other grid constraints (e.g. increased system strength leading to increased short-circuit currents). Mitigation methods can be classified into (i) avoiding the problem (e.g. limiting cable length, avoiding switching scenarios), (ii) suppressing the phenomenon (e.g., using filters) or (iii) adapting the grid components to withstand the phenomenon (e.g. increasing surge arrester ratings).

This report discusses in detail frequency domain assessment methods for background harmonic amplification and (resonant) temporary overvoltages. At present, frequency domain methods are used in practice (i) to estimate harmonic amplification of voltages for grid expansion projects and (ii) in a screening study to find potentially problematic cases concerning temporary overvoltages. The screening study is used to narrow down the number of cases to be assessed in further time domain studies, which are more accurate but also more time consuming. The screening study in the frequency domain finds problematic cases by using limits which are typically based on operational experience or simplified time domain studies.

The report contains eight chapters. In the first chapter a general introduction is given, including industrial reference cases and normative references relevant for resonance analysis. In the second and third chapter, frequency domain calculation methods for and modeling aspects of resonance studies. The fourth chapter elaborates on the interpretation of results as obtained using the frequency domain calculation methods. The fifth chapter introduces the assessment methods as practically used today. In the sixth chapter, mitigation methods for background harmonic amplification and temporary overvoltages are described. The seventh chapter provides an illustration of the frequency domain calculation methods, modeling and result interpretation for resonance analysis in a demonstration grid. The eighth chapter provides the conclusions.

1

Introduction

This report forms part of the project "Resonance and transient behavior of extensive cable grid" and presents a detailed literature review on (i) modelling aspects, (ii) calculation methodologies and their usage in practical studies, (iii) assessment criteria based on the frequency domain results to identify dangerous situations and (iv) mitigation measures related to grid resonances. A case study is included to illustrate the general use of the calculation methodologies and models in order to study frequency shifts.

The report contains eight chapters. In the first chapter a general introduction is given, including industrial reference cases and normative references. In the second chapter, calculation methods for resonance analysis are provided. The third chapter discusses modeling aspects for resonance studies. The fourth chapter elaborates the result interpretation as obtained using the calculation methods. The fifth chapter introduces the assessment methods as practically used today. In the sixth chapter, mitigation measures are described. The seventh chapter provides an illustration of the calculation methods, modeling and result interpretation for a demonstration grid. The eighth chapter provides the conclusions of the report.

1.1 Series and parallel resonances

Power system resonances occur due to the energy exchange between the inductive and capacitive elements within the power system. The introduction of cables into the power system causes an increase in the system capacitance of about twenty times higher than an overhead line of the same length [1]. As a consequence, the resonances in the power system shift to lower frequencies. In general, power system harmonics at lower frequencies are higher in amplitude compared to the ones at higher frequencies. As a consequence, background harmonics in the power system currents present at these lower frequencies may be amplified due to the introduction of cables. Amplified background harmonics may cause voltages and currents in equipment to exceed normal operating ratings, leading to a power quality issues or increased stresses on equipment. Furthermore, during switching events such as component energization, resonance phenomena may occur resulting in temporary overvoltages. Given that, during switching of these elements, the amplitude of low-frequency harmonics is of concern, e.g., in the range of 100-150 Hz, temporary overvoltages may become more severe due to the increase of cables in the system. Temporary overvoltages may lead to instantaneous equipment failure, reduced

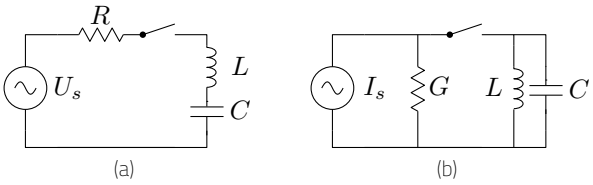

Figure 1.1: Example series (a) and parallel (b) resonance circuits.

lifetime of equipment due to voltages stresses or present hazards to personnel onsite [2].

1.1.1 Series Resonance

Series resonance occurs when a voltage source excites the resonant frequency of a series connected inductive and capacitive element. In the simple example of Fig. 1.1a, taken from [2], the impedance as seen by the source is given by:

$$Z_s = R + j\left(\omega L - \frac{1}{\omega C}\right). \tag{1.1}$$

At the resonant frequency, $\omega L = \frac{1}{\omega C}$ and the impedance becomes R. The current in the circuit is then U_s/R, and the voltages U_L and U_C may reach high amplitudes.

The occurrence of series resonance may be related to interplay between shunt compensation and circuit capacitances (e.g., shunt reactors connected directly to a circuit) or combinations of cables and transformers. Series resonances at fundamental frequency may also occur with (wanted or unwanted) non-synchronized switching of phases in compensated circuits, as interplay between shunt compensation and circuit capacitances [2].

For switching studies, series resonance is normally studied by assessing the resonant frequencies of the circuit and comparing against the frequencies in the switching overvoltage, considering the worst case switching condition [3].

In [4], an example case is studied where a cable energization overvoltage in the high-voltage network is transferred to the low-voltage network as the dominant frequency of the overvoltage matched the natural frequency of the series resonance circuit composed of the cable and the transformer connected at the secondary side. In [5] temporary overvoltages due to series and parallel resonances were studied. The overvoltages due to series resonances were found to be lower than the standard short-duration power-frequency withstand voltage specified in IEC71-1.

1.1.2 Parallel Resonance

Parallel resonance occurs when a current source excites the resonant frequency of a parallel connected inductive and capacitive element. In the simple example of Fig. 1.1b, taken from [2], the admittance seen by the current source is given by:

$$Y_p = G + j\left(\omega C - \frac{1}{\omega L}\right). \tag{1.2}$$

At the resonant frequency, $\omega C = \frac{1}{\omega L}$ and the admittance becomes equal to G. Under these conditions, the currents through the capacitor and inductor take high amplitudes but cancel each other out towards the external network. The voltage on the network components takes a value of I/G, which increases as G decreases.

In [3], potential causes of parallel resonance are transformer energization, cable energization or injection of harmonic frequencies by, e.g., HVDC converters. Transformer energization is considered as the most dangerous one, given high harmonic content, low frequency, low damping and long duration. In particular, parallel resonances around 100 Hz are considered dangerous.

In [6], it is mentioned that parallel resonances can also occur in systems with long HVAC cables, formed by the shunt reactors and the distributed capacitance of the cable.

1.1.3 Impact of cables on resonances

The grid resonances are an interplay between the inductive and capacitive elements in the grid. It may be stated that cables introduce more capacitance into the grid, thereby lowering the resonant frequencies. The general trends associated with cables for varying grid parameters (cable length, grid strength and XR-ratio) are further investigated in [1] in an explorative study and are discussed below in brief.

In [1], the general trends associated with cable resonances are studied. The study considers a cable connected to a grid represented by an equivalent inductance and resistance, representing the grid strength and XR-ratio. In the study, the input impedance (cable input voltage/cable input current), transfer function (cable input vs. cable output current) and output impedance (cable output voltage/cable output current) are calculated. It is concluded that (i) a stronger grid causes a shift of frequency peaks to a higher frequency, but also an increase in magnitude of the peaks, (ii) increasing the cable length lowers the resonance frequency but a decrease in magnitude of the peaks due to the cable resistance, (iii) the sensitivity of the resonance peak magnitudes to the resistive damping is high.

1.2 Resonance Cases in Practice

In the literature, studies and problems associated with resonances due to cables have been reported. The experiences and studies associated with the Danish system are discussed in [7], [8] and [9].

In [7] the high amplitudes of the 11th and 13th harmonic measured in the 15 kV power system of the Anholt island were related to amplification of background harmonics in the 400 kV transmission system. The reason for amplification of background harmonics in the 400 kV system was found in parallel resonance peaks appearing in the frequency spectrum of the equivalent impedance seen from the 400 kV connecting bus.

In [8], experiences from the Danish TSO related to the Horns Rev A and studies for the Horns Rev B wind farms are discussed. The paper indicates that the impedance as seen from the wind farm system is dominated by the cable system, and has a first resonance peak around 140 Hz. Furthermore, the paper analyzes slowly decaying oscillating voltages after disconnecting the wind farm. The paper mentions potential overvoltages when one of the two cable systems (connected in parallel) is disconnected before the other one.

In [9], the 400 kV 60 km Kyndbyværket – Asnæsværket Line is investigated for overvoltages due to series and parallel resonance. A guideline is given for assessing overvoltages for both types of resonance. For series resonance, a guideline for calculating the dominant frequencies in the overvoltages are proposed, as also documented in [4].

The experiences of the French TSO RTE with long EHVAC insulated cables are published by Vernay *et al.* in [10]. The authors report that as a result of the resonances, existing 3^{rd} and 5^{th} background harmonics are amplified up to 20 times. The harmonic studies were carried out using field measurements and simulations in EMTP-RV. To determine harmonic amplifications in future projects, RTE calculates a voltage gain of the future grid situation to the existing grid situation. To assess the harmonics in the future grid situation, the background harmonics measured in the system are multiplied by the calculated gain.

In [5] a study concerning temporary overvoltages due to series and parallel resonances was done for an increased penetration of cables in the Ireland system. It is mentioned that a transformer failure was experienced during test energization by TEPCO, due to an overvoltage caused by series resonance. For the Irish system, overvoltages due to series resonance were analyzed by energizing the 220 kV from the 400 kV system. In this case, no overvoltages exceeding any equipment limit were found. However, an extreme case of parallel resonance (during black start) was found (yet not documented in the report). To analyze overvoltages due to parallel resonance, a frequency scan was performed for various source impedances, cable compensation rates and cable lengths. Based on this study, EMT-type simulations were performed to analyze overvoltages following switching actions. It was found that in certain cases, the surge arrester energy absorption capability was exceeded.

The maximum cable length to be inserted in the 400 kV or 220 kV West-Grid project is assessed by EirGrid in [11]. The authors propose a methodology in consecutive steps, including network modeling, reactive power compensation, scenario selection, frequency scan and time domain simulations. An assessment criterion based on TOV withstand capability is discussed. The authors conclude that in the 400 kV system, a 10 km cable is not acceptable, and a tuned filter at around 150 Hz would be required to mitigate overvoltages due to switching actions for 23 to 30 km of cable in the 220 kV grid.

In The Netherlands, the challenges associated with cable systems were tackled in the Dutch cable research program. The Dutch cable research program led to several PhD theses related to resonant and transient behavior of cable grids, amongst them [12, 13, 14, 15]. The Dutch TSO TenneT also conducted frequency scan studies in DIgSILENT Power Factory and ATP-EMTP to reveal a resonance around 125 Hz due to the foreseen connection of offshore wind farms to the 380 kV network via long offshore cables [16].

In [17], the harmonic impedances and mitigation techniques for a system expansion with cables in Connecticut were analyzed. The conclusions were (i) additional cables lead to lower resonance frequencies, (ii) resonance points below the third harmonic were possible with certain grid expansions (and were considered risky), (iii) a combination of C-type filters and STATCOMs could be used as mitigation techniques and (iv) transient analyses with detailed system models are recommended.

The majority of studies on switching overvoltages focus on the introduction of parallel resonances around 100-200 Hz due to the insertion of long cables, and consider these cases potentially problematic for switching overvoltages or fault recovery. In [5], recommendations are to avoid switching in networks with parallel resonance peaks close to 100 Hz. In [18], thresholds are set on the impedances around 100-200 Hz to identify cases to for further investigation. In [17], 150 Hz is considered as a border frequency below which ideally no resonance peaks occur. In [11], a case with a peak around 150 Hz was investigated and was shown to lead to unacceptable overvoltages.

1.3 Normative References and Guidelines

1.3.1 Normative References

IEEE 399 IEEE Std. 399 is the "IEEE Recommended Practice for Industrial and Commercial Power Systems Analysis (Brown Book)". It provides multiple studies and guidance for the preparation of these studies. Some of the studies discussed are: load flow studies, short-circuit studies, stability studies, motor starting studies, harmonic analysis studies, switching transient studies, reliability studies, cable ampacity studies, ground mat studies, coordination studies, and dc auxiliary power system analyses.

IEEE 519 IEEE Std. 519 has the title "Recommended Practices and Requirements for Harmonic Control in Electrical Power Systems". The version of 2004 [19] contains a part on harmonic measurements and a part on recommended harmonic voltage and current distortion limits. The version of 1992 [20] is more elaborate, e.g., there is a section on modeling, but information may be outdated.

IEEE 1531 IEEE Std. 1531 - 2003 (R2009) is the "IEEE Guide for Application and Specification of Harmonic Filters". It specifies design considerations for harmonic filters in general and gives specific recommendations for filter design for low-, medium- and high-voltage filters.

IEEE 3002.8-2018 is the "Recommended Practice for Conducting Harmonic Studies and Analysis of Industrial and Commercial Power Systems". It describes methodology for harmonic analysis, system simulation and modeling, required input data, data collection and preparation and gives recommendations for study scenarios, solution parameters and results. The standard particularly focuses on industrial and commercial power systems, although the basics also apply to high-voltage systems. The standard focuses on steady-state harmonics rather than time-varying harmonics.

IEC 61000 IEC 61000 provide according to [ArrillagaBook] internationally accepted information for the control of power system harmonic (and inter-harmonic) distortion. It mainly discusses electromagnetic compatibility (EMC).

IEC TR60071-4 IEC TR60071-4:2004 is a "Computational guide to insulation co-ordination and modeling of electrical networks". It classifies parallel line resonance as a temporary overvoltage and provides modeling guidelines. It also presents a method for a fast estimate on temporary overvoltages and a detailed calculation method.

1.3.2 Guidelines

CIGRE TB139 The second chapter of the addendum to CIGRE TB139 [21] from WG B4.47 (Guide to the specification and design evaluation of AC filters for HVDC systems) discusses considerations for network modeling and selecting case studies for AC filter design for HVDC systems. The appendix of this chapter also contains information on AC network impedance modeling for harmonic frequencies, focusing on loads, transformers, machines and transmission lines.

CIGRE TB556 This technical brochure [6] discusses technical performance issues related to long AC cables, and gives modeling recommendations for cables for power frequency and transient studies.

CIGRE TB568 This technical brochure [22] provides a generic guidance on transformer energization studies in power systems. In particular, it discusses the problems associated with overvoltages as a result of parallel resonances during transformer energization. It also provides an overview of mitigation measures and best practices associated with these overvoltages.

CIGRE TB569 This technical brochure [2] discusses the fundamentals of resonance and ferroresonance in power networks, introduces typical topologies and gives modeling recommendations mainly for resonance at fundamental frequency and ferroresonance.

CIGRE TB766 This technical brochure [23], released in April 2019, contains extensive up-to-date information on network modeling for harmonic studies. Besides passive elements, it also dedicates a chapter to power-electronic based network elements.

CIGRE TB754 CIGRE TB754 discusses harmonic aspects with VSC HVDC systems. It discusses the VSC as source of harmonics and proposes modeling methods for VSCs in harmonic studies. In the brochure, harmonic instabilities due to control interactions (e.g., non-passivity) of the VSC with the grid impedance are also discussed.

CIGRE WGB4.66 CIGRE WGB4.66 (TB number to be assigned) discusses the coordinated design of harmonic filters for HVDC converter station in close proximity. It discusses aspects such as filter rating, identification and prevention of potentially problematic resonances and specification of harmonic limits applied to this particular case. For instance, it recommends a harmonic interaction screening based on (harmonic) multi-infeed interaction factors.

2

Calculation Methods

This chapter introduces the calculation methods that can be used for a frequency-domain assessment of resonances and harmonics. It mainly details the rationale behind the calculation methods. Chapter 4.5 details the interpretation of the results of these calculation methods and provides a comparison of when to use which method.

2.1 Preliminary Analysis

In [1], a simplified calculation method is used in a preliminary analysis. The resonant frequency is estimated based on:

$$f_r = \frac{1}{2\pi\sqrt{LC}}, \tag{2.1}$$

where L is calculated based on the short-circuit power of the grid connected to the cable and C is the total cable capacitance. This method is also used in IEEE Std. 519-1992 [20] in a preliminary analysis concerning capacitors.

The drawbacks of this method is that (i) it ignores frequency-dependent effects in the impedance of the feeding grid, and (ii) it ignores distributed effects in the cable capacitance and (iii) it lumps all of the capacitance at a single point. In [24], it is concluded that this method is too crude to be practical even for resonance calculations with capacitor banks. In cable applications, the errors by this method were found to grow larger for long cables connected to strong grids [1].

In [9], a similar simple calculation method is given for a cable which is modeled using distributed parameters. The resonance frequency of such a cable is given by:

$$f_r = \frac{1}{4\sqrt{LC}}, \tag{2.2}$$

where L and C are the total inductance and capacitance of the cable.

We recommend to use these methods only in a preliminary analysis to identify the range of frequencies potentially introduced by the cable system.

2.2 Frequency Scan

A frequency scan analysis provides the "input" impedance at the injection bus or "transfer" impedance from the injection bus to the test bus for each frequency. The input impedance at node k is calculated as the relationship between the current injected at node k, considering all other current injections zero, and the resulting voltage at node k. The transfer impedance from node k to node l is considered as the relationship between the current injected at node k, considering all other current injections as zero, and the resulting voltage at node l. With injection bus, the bus at which the harmonic current is injected is meant, whereas with test bus, the bus at which the harmonic voltage is evaluated is meant.

2.2.1 Admittance Matrix

In this case, the input and transfer impedances are calculated by first calculating the admittance matrix Y. The admittance matrix Y can be constructed based on the network topology and the primitive admittance matrices of each component.

For an N-node network, for each frequency ω_n, the relationship between currents injected at the nodes $\{I_1(\omega_n), \ldots I_N(\omega_n)\}$ and voltages on the nodes $\{U_1(\omega_n), \ldots U_N(\omega_n)\}$ is given by

$$\begin{bmatrix} I_1(\omega_n) \\ I_2(\omega_n) \\ \vdots \\ I_k(\omega_n) \\ \vdots \\ I_N(\omega_n) \end{bmatrix} = \begin{bmatrix} Y_{1,1}(\omega_n) & Y_{1,2}(\omega_n) & \cdots & Y_{1,k}(\omega_n) & \cdots & Y_{1,N}(\omega_n) \\ Y_{2,1}(\omega_n) & Y_{2,2}(\omega_n) & \cdots & Y_{2,k}(\omega_n) & \cdots & Y_{2,N}(\omega_n) \\ \vdots & \vdots & \ddots & \vdots & \ddots & \vdots \\ Y_{k,1}(\omega_n) & Y_{k,2}(\omega_n) & \cdots & Y_{k,k}(\omega_n) & \vdots & Y_{k,N}(\omega_n) \\ \vdots & \vdots & \ddots & \vdots & \ddots & \vdots \\ Y_{N,1}(\omega_n) & Y_{N,2}(\omega_n) & \cdots & Y_{N,k}(\omega_n) & \cdots & Y_{N,N}(\omega_n) \end{bmatrix} \begin{bmatrix} U_1(\omega_n) \\ U_2(\omega_n) \\ \vdots \\ U_k(\omega_n) \\ \vdots \\ U_N(\omega_n) \end{bmatrix}, \tag{2.3}$$

where $Y_{x,y}(\omega_n)$ is the matrix element at position x, y in the admittance matrix $Y(\omega_n)$ at frequency ω_n. In the following, the argument ω_n is omitted for brevity of notation, thereby implicitly assuming that all quantities are calculated at a certain frequency.

The impedance matrix can then be calculated as the inverse of the admittance matrix:

$$Z = Y^{-1}. \tag{2.4}$$

The on-diagonal entries represent the "input-" or "self-impedances", i.e., the Thévenin impedance of the network as seen from bus k. The off-diagonal entries represent the "transfer" or "mutual" impedances. The harmonic voltage at a bus l for an injection of 1.0 A with a harmonic frequency of h at bus l can thus be found as the amplitude of $Z_{h,k,l}$.

Alternatively, the input impedance can be calculated using following steps. First, the voltage at node k is put at the first row of the voltage vector U. This requires changing columns 1 and k:

$$\begin{bmatrix} 0 \\ 0 \\ \vdots \\ I_k \\ \vdots \\ 0 \end{bmatrix} = \begin{bmatrix} Y_{1,k} & Y_{1,2} & \cdots & Y_{1,1} & \cdots & Y_{1,N} \\ Y_{2,k} & Y_{2,2} & \cdots & Y_{2,1} & \cdots & Y_{2,N} \\ \vdots & \vdots & \ddots & \vdots & \ddots & \vdots \\ Y_{k,k} & Y_{k,2} & \cdots & Y_{k,1} & \vdots & Y_{k,N} \\ \vdots & \vdots & \ddots & \vdots & \ddots & \vdots \\ Y_{N,k} & Y_{N,2} & \cdots & Y_{N,1} & \cdots & Y_{N,N} \end{bmatrix} \begin{bmatrix} U_k \\ U_2 \\ \vdots \\ U_1 \\ \vdots \\ U_N \end{bmatrix} \tag{2.5}$$

Thereafter, rows 1 and k are changed as to put I_k at the first row of the current vector I:

$$\begin{bmatrix} I_k \\ 0 \\ \vdots \\ 0 \\ \vdots \\ 0 \end{bmatrix} = \begin{bmatrix} Y_{k,k} & Y_{k,2} & \cdots & Y_{k,1} & \cdots & Y_{k,N} \\ Y_{2,k} & Y_{2,2} & \cdots & Y_{2,1} & \cdots & Y_{2,N} \\ \vdots & \vdots & \ddots & \vdots & \ddots & \vdots \\ Y_{1,k} & Y_{1,2} & \cdots & Y_{1,1} & \cdots & Y_{1,N} \\ \vdots & \vdots & \ddots & \vdots & \ddots & \vdots \\ Y_{N,k} & Y_{N,2} & \cdots & Y_{N,1} & \cdots & Y_{N,N} \end{bmatrix} \begin{bmatrix} U_k \\ U_2 \\ \vdots \\ U_1 \\ \vdots \\ U_N \end{bmatrix} \tag{2.6}$$

The admittance matrix is now in the format of:

$$\left[\begin{array}{c|c} Y_{k,k} & Y_{k,:} \\ \hline Y_{:,k} & Y_{:,:} \end{array}\right], \tag{2.7}$$

and Kron elimination can be applied to find the equivalent admittance seen from bus k:

$$Y_k = Y_{k,k} - Y_{k,:} Y_{:,:}^{-1} Y_{:,k}. \tag{2.8}$$

The input impedance can be calculated as the inverse of Y_k:

$$Z_{h,k,k} = Y_k^{-1}. \tag{2.9}$$

The transfer impedance from node k to node l can be obtained via a similar routine, where instead of U_k, U_l is swapped with the first row.

2.2.2 ABCD Matrix

The ABCD matrix presents an alternative approach for representing multiport network. Each subnetwork of the multiport network can be represented using ABCD parameters between chosen input pins (nodes) and output pins (nodes). Input and output nodes are described by their voltage and current. Thus, ABCD parameters provide a connection between input voltages and currents and output voltages and currents. Let us assume that with $V_{i,k}$ and $I_{i,k}$ are denoted as the k-th multiport input voltage and current, and with $V_{o,k}$ and $I_{o,k}$ the k-th output voltage and current, respectively. In case of N input and N output nodes, the ABCD parameters result in the following matrix relation:

$$\begin{bmatrix} V_{i,1} \\ V_{i,2} \\ \vdots \\ V_{i,N} \\ I_{i,1} \\ \vdots \\ I_{i,N} \end{bmatrix} = \begin{bmatrix} A_{1,1} & A_{1,2} & \cdots & A_{1,N} & B_{1,1} & B_{1,2} & \cdots & B_{1,N} \\ A_{2,1} & A_{2,2} & \cdots & A_{2,N} & B_{2,1} & B_{2,2} & \cdots & B_{2,N} \\ \vdots & \vdots & \ddots & \vdots & \vdots & \vdots & \ddots & \vdots \\ A_{N,1} & A_{N,2} & \cdots & A_{N,N} & B_{N,1} & B_{N,2} & \cdots & B_{N,N} \\ C_{1,1} & C_{1,2} & \cdots & C_{1,N} & D_{1,1} & D_{1,2} & \cdots & D_{1,N} \\ \vdots & \vdots & \ddots & \vdots & \vdots & \vdots & \ddots & \vdots \\ C_{N,1} & C_{N,2} & \cdots & C_{N,N} & D_{N,1} & D_{N,2} & \cdots & D_{N,N} \end{bmatrix} \begin{bmatrix} V_{o,1} \\ V_{o,2} \\ \vdots \\ V_{o,N} \\ I_{o,1} \\ \vdots \\ I_{o,N} \end{bmatrix}. \tag{2.10}$$

Usually this matrix is represented by its $N \times N$ sized submatrices $\mathbf{A}$, $\mathbf{B}$, $\mathbf{C}$ and $\mathbf{D}$:

$$\begin{bmatrix} V_{i,1} \\ V_{i,2} \\ \vdots \\ V_{i,N} \\ I_{i,1} \\ \vdots \\ I_{i,N} \end{bmatrix} = \begin{bmatrix} \mathbf{A} & \mathbf{B} \\ \mathbf{C} & \mathbf{D} \end{bmatrix} \begin{bmatrix} V_{o,1} \\ V_{o,2} \\ \vdots \\ V_{o,N} \\ I_{o,1} \\ \vdots \\ I_{o,N} \end{bmatrix}, \tag{2.11}$$

whose components have values $X_{i,j}$ for $X \in \{A, B, C, D\}$ and $i, j \in \{1, \cdots, N\}$ as in (2.10).

Although ABCD parameters can only be properly defined when the number of input and output nodes (voltages and currents) is the same, this multiport representation has multiple advantages:

- The input and output multiport impedance can be found directly. The impedance visible from the input nodes, assuming that output nodes are attached to the diagonal load $\tilde{\mathbf{Z}}_t$ or "grounded" (represented by a zero load matrix), is given with the formula:

  $$\mathbf{Z}_i = (\mathbf{A}\tilde{\mathbf{Z}}_t + \mathbf{B})(\mathbf{C}\tilde{\mathbf{Z}}_t + \mathbf{D})^{-1}, \tag{2.12}$$

  while the impedance visible from the multiport output nodes with attached to the diagonal load or "grounded" input nodes is:

  $$\mathbf{Z}_o = (\tilde{\mathbf{Z}}_t \times \mathbf{C} - \mathbf{A})^{-1} \times (\tilde{\mathbf{Z}}_t \times \mathbf{D} - \mathbf{B}). \tag{2.13}$$

- There is the unique representation of the each multiport network using ABCD parameters. For instance, ABCD parameters are defined even in cases where the admittance matrix does not exist, e.g., in case of a infinite shunt admittance.

- ABCD parameters operate with voltages and currents and thus, the values inside ABCD matrix have clear physical dimension and "meaning". This cannot be said for H (hybrid) parameters, which is usually used for RF and microelectronics simulations.
- There is a unique relationship between multiport Z, Y, H, S and ABCD multiport parameters [25, 26].

In power systems, the ABCD representation is at the moment not widely used in simulation tools. However, taking in the account that "natural" frequency dependent transmission line model is given using ABCD parameters, the use of ABCD parameters in power system analysis and simulation is becoming a popular topic. Research presented in [12] proposes the use of ABCD parameters for simulation of the power system network containing both overhead lines and cables.

2.2.3 Fast Fourier Transform

Besides an analytical approach, the input or transfer impedance at a specific harmonic frequency can be obtained using a time-domain simulation in an EMT-type tool by injecting a harmonic current at an injection bus k and measuring the resulting voltage at the test bus l. The impedance is obtained by applying the Fast Fourier Transform (FFT) to the voltage measured at the test bus and the current injected at the injection bus:

$$Z_{h,k,l} = \frac{V_l(h)}{I_k(h)}. \tag{2.14}$$

2.3 Harmonic Resonance Mode Analysis

A tool mainly developed for parallel resonance analysis was introduced in 2005 by Wilsun Xu et al [27], and uses eigenvector analysis on the admittance matrix bus to find the modal response of the system. The benefit of using Resonance Mode Analysis (RMA) over a frequency scan of the admittance matrix is that it may provide information on which buses or devices are contributing to certain resonances, which cannot be obtained using a frequency scan.

In RMA, the admittance matrix Y is decomposed into left, L, and right eigenvectors, R, and a diagonal matrix containing the eigenvalues Λ:

$$[Y] = [L][\Lambda][R]. \tag{2.15}$$

Defining $[U_m] = [R]U$ and $[I_m] = [L]I$ as the vectors of voltages and currents in the modal domain gives:

$$[U_m] = [\Lambda]^{-1}[I_m], \tag{2.16}$$

and in full:

$$\begin{bmatrix} U_{m,1} \\ U_{m,2} \\ \vdots \\ U_{m,N} \end{bmatrix} = \begin{bmatrix} \lambda_1^{-1} & 0 & \cdots & 0 \\ 0 & \lambda_2^{-1} & \cdots & 0 \\ \vdots & \vdots & \ddots & \vdots \\ 0 & 0 & \cdots & \lambda_N^{-1} \end{bmatrix} \begin{bmatrix} I_{m,1} \\ I_{m,2} \\ \vdots \\ I_{m,N} \end{bmatrix} \tag{2.17}$$

It can be seen from the diagonal matrix that if the modal impedance is equal to zero, i.e., $\lambda_1 = 0$, or approaches a singularity, a small modal current, J_1, would lead to a large modal voltage, U_1. A low value for λ thus can be used to identify a parallel resonance. In [27], the smallest eigenvalue is denoted as the critical mode and its eigenvectors as the critical eigenvectors.

The critical right and left eigenvectors indicate the locational "excitability" and the locational "observability" of the critical mode. For instance, consider the modal current of the first mode as critical mode:

$$I_{m,1} = R_{11}I_1 + R_{12}I_2 + \ldots + R_{1N}I_N. \tag{2.18}$$

It can be seen that the value of R_{1k} determines the contribution of a bus to the first mode. The modal voltage can be distributed over the buses as:

$$\begin{bmatrix} U_1 \\ U_2 \\ \vdots \\ U_N \end{bmatrix} = \begin{bmatrix} L_{11} \\ L_{21} \\ \vdots \\ L_{N1} \end{bmatrix} U_{m,1} + \begin{bmatrix} L_{12} \\ L_{22} \\ \vdots \\ L_{N2} \end{bmatrix} U_{m,2} + \cdots + \begin{bmatrix} L_{1N} \\ L_{2N} \\ \vdots \\ L_{NN} \end{bmatrix} U_{m,N}. \tag{2.19}$$

The contribution of a certain mode m to a certain bus k is thus given by $L_{k,m}$, or in other words, a large value of $L_{k,m}$ implies that mode m can be easily observed at bus k. If mode 1 is the critical mode, the above equation reduces to:

$$\begin{bmatrix} U_1 \\ U_2 \\ \vdots \\ U_N \end{bmatrix} \approx \begin{bmatrix} L_{11} \\ L_{21} \\ \vdots \\ L_{N1} \end{bmatrix} U_{m,1}. \tag{2.20}$$

In [27], it is also noted that the critical mode may not produce harmful behavior, but it is not investigated how the magnitude of the modal impedance may be related to any harmful behavior.

The benefit of using modal analysis is thus in identifying the locational observability and excitability of resonances, which may be done using a participation factor. Participation factors of the bus to the critical mode are defined as $PF_{m,k} = L_{m,k}R_{m,k}$, and these combine observability and excitability. A relationship utilized in [27] is that $[R] = [L]^T$, which leads to two interesting conclusions:

1. The bus where the modal resonance is the most observable is also the bus that contributes the most to the modal resonance.

2. Participation factors are equal to the square of the eigenvectors, meaning that either participation factor or eigenvectors are needed for the analysis. The participation factors may thus be used as an index on how far the resonance will propagate. The bus with the highest participation factor is considered as "center of resonance".

It is important to note that this method may not be used to analyze series resonances. To identify a series resonance, one should define a loop impedance matrix, and analyze the inverse of the eigenvalues of this matrix.

2.4 Voltage Scan

A voltage scan calculates the voltage gain of a voltage measured at bus l to the current injected at bus k. The voltage gain is thus defined by:

$$G(\omega) = \frac{U_l(\omega)}{U_k(\omega)}. \tag{2.21}$$

2.4.1 Matrix Method

The voltage gain may be calculated by considering an injection bus k and test bus l as follows. A voltage is injected at buses k, whereas the other buses are open-circuited:

$$\begin{bmatrix} 0 \\ \vdots \\ I_k \\ \vdots \\ 0 \\ \vdots \\ 0 \end{bmatrix} = \begin{bmatrix} Y_{1,1} & \cdots & Y_{1,k} & \cdots & Y_{1,l} & \cdots & Y_{1,N} \\ \vdots & \ddots & \vdots & \ddots & \vdots & \ddots & \vdots \\ Y_{k,1} & \cdots & Y_{k,k} & \cdots & Y_{k,l} & \cdots & Y_{k,N} \\ \vdots & \ddots & \vdots & \ddots & \vdots & \ddots & \vdots \\ Y_{l,1} & \cdots & Y_{l,k} & \cdots & Y_{l,l} & \cdots & Y_{l,N} \\ \vdots & \ddots & \vdots & \ddots & \vdots & \ddots & \vdots \\ Y_{N,1} & \cdots & Y_{N,k} & \cdots & Y_{N,l} & \cdots & Y_{N,N} \end{bmatrix} \begin{bmatrix} U_1 \\ \vdots \\ U_k \\ \vdots \\ U_l \\ \vdots \\ U_N \end{bmatrix}. \tag{2.22}$$

From the l-th row, we can deduces the relationship between the voltages injected at k and measured at l:

$$G_{k,l}(\omega) = -\frac{Y_{l,k}}{Y_{l,l}}. \tag{2.23}$$

2.4.2 Fast Fourier Transform

Similar to the frequency scan, an FFT can be applied to the voltages obtained using an EMT-simulation, in which a harmonic voltage is injected at bus k and the voltage is measured at bus l.

2.5 Background Harmonic Amplification Calculation

In [10, 28, 18], methods are proposed to calculate the background harmonic amplification due to a grid investment project.

In [10, 28], the way to calculate voltage gains is as follows. The voltage at a certain location and a certain harmonic, $\boldsymbol{U(h)}_{\text{ref}}$ is calculated using the existing grid topology, for a 1A current injection at a certain point. The same voltage is calculated for the grid post-investment, and labelled $\boldsymbol{U(h)}_{\text{post}}$. The voltage gain is then calculated as:

$$G(h) = \frac{U(h)_{\text{post}}}{U(h)_{\text{ref}}}. \tag{2.24}$$

To calculate the expected value of the harmonic voltage, the gain may be multiplied by the voltage measured at that location. In [28], mainly a radial connection is considered, and only 1 current source injection.

The first option mentioned in [18] is to calculate the voltage gain for a voltage injected behind a certain grid impedance. This may be done using, e.g., a voltage scan. This is, e.g., the approach followed in [7]. In [18], it is mentioned that this option is mainly suitable for radial grids.

The second option mentioned in [18] is to calculate the voltage gain similar to , but now using multiple harmonic current injections (at different locations). For each current injection, the voltage at a certain location is calculated (e.g., termed $\boldsymbol{U(h)_{xy}}$, with $\boldsymbol{x}$ the bus at which the voltage is calculated and $\boldsymbol{y}$ the location at which the current is injected). Given that the relative phases of the harmonic current injections are unknown, the summation law as described in IEC 61000-3-6 is used:

$$U(h)_x = \left(\sum_{y=1}^{N} (U(h)_{xy})^{\alpha} \right)^{1/\alpha} \tag{2.25}$$

It should be noted that, if each current source is treated individually, $\boldsymbol{U(h)_{xy} = Z_{xy} I_y}$, or in other words, $\boldsymbol{U(h)_x}$ is a generalized mean of the harmonic impedances of the $\boldsymbol{x}$-th row by the estimated amplitudes of the harmonic current sources $\boldsymbol{I_y}$.

2.6 Implementations in Commercial Software Tools

All references to the calculation methods and models found in software tools are based on [29] and the online help for PSCAD,the DigSilent Manual of 2019 [30], and the SinCal manual of 2016 [31] unless stated otherwise.

2.6.1 DigSilent PowerFactory

DigSilent PowerFactory offers the possibility to analyze harmonics in the frequency domain, through (i) a harmonic load flow, and (ii) a frequency sweep.

The harmonic load flow calculates the steady-state solution for voltages and currents at a certain frequency, considering harmonic current and voltages sources. Harmonic sources can be defined within certain components. Based on the results, harmonic indices (e.g., total harmonic distortion,...) can be requested as an output.

The frequency sweep calculates the "input" and "transfer" impedances in the frequency domain, as well as the response of any variable to a step or impulse function. The frequency sweep may be done for a balanced or unbalanced network configuration.

2.6.2 PSCAD

PSCAD offers the possibility to analyze harmonics in the frequency or time domain.

The frequency scan tool (Harmonic Impedance Solution/Frequency Scanner) available in PSCAD builds the system admittance matrix based only on the passive elements in the system. It further uses following assumptions:

1. Transformers and surge arresters operate in unsaturated region.
2. Power electronic devices are assumed in their off-state.
3. Machines are represented by a grounded inductor.

4. The 0-sequence impedance of an SVC is represented as the primary-delta leakage reactance of the transformer, and the +/- sequence impedance is represented by the defined shunt loss conductance.

5. The minimum frequency is 1 μHz.

The frequency scan tool is said to only consider passive elements, and not consider effects of controls (if any) [32].

An approach to incorporate control effects was used in [32], where the FFT approach as outlined in Section 2.2.3 was used to obtain the frequency response.

2.6.3 SinCal

SinCal first calculates the admittance matrix based on the inputs. Using this admittance matrix, it calculates the voltages at each node for each frequency, assuming a 1A input current at the so-called reference node k. The resulting impedances $Z_{l,k}$ are found as $\frac{U_l}{I_k}$.

3

Models

Several sources stress the importance of correct modeling of the network and network components. A too conservative approach may lead to overly severe mitigation methods to be applied, whereas a too loose approach may result in unforeseen problems, as mentioned in [21] for harmonic filter design for HVDC applications.

With respect to network models, following must be accounted for [21]:

- Accuracy of network component data
- Limitations of component impedance models in frequency domain
- Variation of component impedances with ambient and system conditions.

The frequency-dependent nature of the component parameters (e.g., transmission line or transformer resistance) must be taken into consideration when performing a harmonic analysis [23]. It it is therefore important to note that data at the fundamental frequency, although in general easily available, may not be sufficient to model components with sufficient accuracy for the whole frequency range of the study. By contrast, the accuracy of frequency-dependent component models must be assessed within the range of the study [21].

In this chapter, the different component models are discussed and modeling guidelines are formulated. In accordance with the project scope, emphasis is put on the modeling of passive components and the topic of modeling power-electronic components is touched upon.

3.1 Transmission Lines

Both cables and overhead lines are being described using Telegrapher's equation or wave propagation equation, whose solution is frequency dependent and especially suitable for the component representation using multiport parameters.

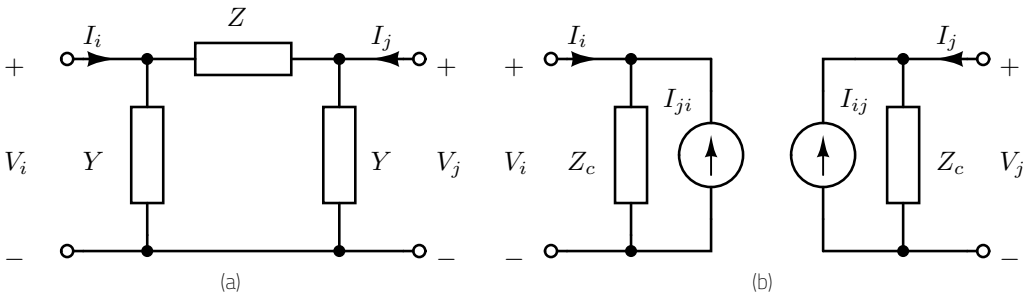

Figure 3.1: Frequency-domain (a) and time-domain (b) model structure.

The voltage and current drop along an infinitesimal short line can be written as [33]:

$$\begin{aligned} \frac{d\boldsymbol{V}(x,\omega)}{dx} &= -\boldsymbol{Z}(\omega)\ \boldsymbol{I}(x,\omega), \\ \frac{d\boldsymbol{I}(x,\omega)}{dx} &= -\boldsymbol{Y}(\omega)\boldsymbol{V}(x,\omega), \end{aligned} \tag{3.1}$$

based on which the wave propagation equation can be written as:

$$\begin{aligned} \frac{d\boldsymbol{V}^2(x,\omega)}{dx^2} &= \boldsymbol{Z}(\omega)\boldsymbol{Y}(\omega)\ \boldsymbol{V}(x,\omega), \\ \frac{d\boldsymbol{I}^2(x,\omega)}{dx^2} &= \boldsymbol{Y}(\omega)\boldsymbol{Z}(\omega)\boldsymbol{I}(x,\omega). \end{aligned} \tag{3.2}$$

(3.3)

In the above equations, the per unit series impedance and shunt admittance are given by $\boldsymbol{Z}(\omega) = \boldsymbol{R}(\omega) + j\omega\boldsymbol{L}(\omega)$ and $\boldsymbol{Y}(\omega) = \boldsymbol{G} + j\omega\boldsymbol{C}$ and are typically frequency-dependent. The voltage and current at a given point $\boldsymbol{x}$ along the line can be written in the format of:

$$\boldsymbol{I}_x(\omega) = e^{-\boldsymbol{\gamma} l}\boldsymbol{I}_f(\omega) + e^{\boldsymbol{\gamma} l}\boldsymbol{I}_b(\omega) \tag{3.4}$$

$$\boldsymbol{V}_x(\omega) = \boldsymbol{Y}_c\left(e^{-\boldsymbol{\gamma} l}\boldsymbol{I}_f(\omega) - e^{\boldsymbol{\gamma} l}\boldsymbol{I}_b(\omega)\right) \tag{3.5}$$

, in which $\boldsymbol{Y}_c = \boldsymbol{Z}^{-1}\sqrt{\boldsymbol{ZY}}$ and $\boldsymbol{\gamma} = \sqrt{\boldsymbol{ZY}}$. This yields a format which is suitable to derive Norton equivalent transmission line circuits which relate input and output voltages and currents in a time domain simulation:

$$\boldsymbol{I}_o(\omega) = \boldsymbol{Y_c}\boldsymbol{V}_o(\omega) - \boldsymbol{H}(\boldsymbol{Y}_c\boldsymbol{V}_i(\omega) + \boldsymbol{I}_i(\omega)) \tag{3.6}$$

$$\boldsymbol{I}_i(\omega) = \boldsymbol{Y_c}\boldsymbol{V}_i(\omega) - \boldsymbol{H}(\boldsymbol{Y}_c\boldsymbol{V}_o(\omega) + \boldsymbol{I}_o(\omega)). \tag{3.7}$$

The solution to the transmission line equations can also be written as a relation between input (sending end) and output (receiving end) voltages and currents:

$$\begin{bmatrix}\boldsymbol{V}_i \\ \boldsymbol{I}_i\end{bmatrix} = \begin{bmatrix}\cosh(\boldsymbol{\gamma} l) & (\boldsymbol{Y}_c)^{-1}\sinh(\boldsymbol{\gamma} l) \\ \boldsymbol{Y}_c\sinh(\boldsymbol{\gamma} l) & \cosh(\boldsymbol{\gamma} l)\end{bmatrix}\begin{bmatrix}\boldsymbol{V}_o \\ \boldsymbol{I}_o\end{bmatrix}, \tag{3.8}$$

yielding a format which is suitable for frequency domain simulations.

3.1.1 Model Types

Relevant information related to modeling of transmission lines may be in Commercial [34, 3, 35]. In general, line models may be categorized in frequency-domain (Fig.) and time-domain models (Fig.).

Frequency-domain Models

Matrix format Depending on the analysis, the frequency domain relationship may be in the format of (3.8), known as the chain matrix, or in an admittance, impedance or hybrid matrix format.

Equivalent PI model Based on (3.8), an equivalent PI model can be derived, in which the series impedance is given by $(Zl)\frac{\sinh\gamma l}{\gamma l}$ and the shunt admittance is given by $(Yl)\frac{\tanh\gamma l/2}{\gamma l/2}$. This circuit representation is an exact representation of the transmission line for a given frequency [34].

Nominal PI model The nominal PI model is a single frequency representation of the equivalent PI model. The validity of the approximation depends on the frequencies of interest.

Cascaded PI model The cascaded PI-model approximates the hyperbolic part of the frequency dependence of the series and shunt admittance of the equivalent PI-model. Increasing the number of cascaded sections may increase the model accuracy compared with the nominal PI-model. However, this model has limits as the frequency-dependence is only partly taken into account [34].

Time-domain Models

PI-models The nominal and cascaded PI model as described above may be implemented for time-domain simulations. As these models provide none to limited frequency-dependency, behavior may be incorrect for time-domain simulations.

Bergeron model The Bergeron model is a time-domain single-frequency distributed parameter model. It represents the transmission line by a lossless characteristic impedance and a single propagation constant. The propagation constant relates the traveling waves at the sending end to the receiving end. The Bergeron model may take into account losses by means of lumped resistances [34].

Marti The JMarti (or frequency-dependent mode model, FD-line model) is a time-domain frequency-dependent distributed parameters model [36]. It uses a real and constant (frequency-independent) modal transformation applied to the propagation constant $e^{\gamma l}$ and the characteristic admittance Y_c, to obtain their counterparts in the modal domain. These values in the modal domain may be synthesized using RC circuits or are fitted using rational functions, such that convolutions in the time domain may be efficiently carried out. In a time domain simulation, all phase-domain values are thus first transformed to the modal domain, then the line model is executed, and modal domain values are converted back into the phase domain. This model is accurate only for geometrically balanced transmission lines [29]. An extension is the LMarti model or FDQ model, which uses frequency-dependent modal transformation matrices.

ULM The universal line model (or frequency-dependent phase model) is a time-domain frequency-dependent distributed parameters model [37]. It uses rational fitting applied directly to the propagation constant and characteristic admittance in the phase domain. The sole loss of accuracy in this model hence lies in the rational fitting. This type of model thus retains accuracy even for unbalanced transmission line configurations. This model is today's model of choice in commercial EMT-type tools.

3.1.2 Overhead lines

The series impedance and shunt admittance of overhead lines are calculated by line constants routines based on the tower geometry and material parameters of the conductors and the earth. The overhead line (OHL) configuration and calculation of the parameters are described in detail in [33, 29].

Modeling Guidelines

Transmission line modeling guidelines are summed in the CIGRE WG brochures [38, 23] and in the standard IEC TR 60071-4 [39]. This section summarizes the findings in these references, based on the structure provided in [23].

Transmission line model In frequency domain studies, as the model does not provide a lot of overhead, the frequency-dependent models) should always be preferred whenever data is easily available. In remote parts of the system, or at voltage levels lower than the one of interest, a nominal PI model may also provide sufficient accuracy [15, 40].

Skin effect According to [23], skin effect should always be modeled for harmonic studies. The skin effect may be incorporated by equations based on Bessel functions [33] or by approximations as given in [23]. Neglecting skin effect may lead to underestimation of damping in the higher frequency regions, and as such, at resonant frequencies.

Earth resistivity A common practice is to neglect variations of earth resistivity with depth, as to simplify calculations. However, this may introduce errors (especially in the zero-sequence or ground return mode), of which one should be aware. For long circuits, different earth conditions along the line length may be considered.

Distributed Parameter effects Distributed parameter effects should be taken into account except for the shortest lines and for overhead lines remote from the area of interest. The guideline given in [IEEE Task Force] states that lumped parameters may only be used up to $240/h$ km, where h is the harmonic order of interest (and the fundamental frequency is).

Average conductor height OHL conductor average high shows to have small impact of the harmonic circuit impedance [23].

Single- or multiphase models Normative references suggest using multi-phase models whenever there is any asymmetry in the construction of the transmission line.

Models in Commercial Software

PSCAD offers multiple transmission line models, of which the *nominal PI-model, the Bergeron model and the frequency-dependent mode and phase models*. It offers a very modular overhead line model. From the geometry point of view, a different tower organizations are provided, denoted as: flat (horizontal as a flat without ground wires), vertical, delta (for lines with at least three phases), offset (at least three phases), concentric (at least three phases). Conductors can be bundled with both symmetric and asymmetric subconductor positioning. Computationally, both solutions with Bessel function and a variety of the approximations are provided [29].

DigSilent PowerFactory DigSilent PowerFactory offers (i) distributed parameters (*equivalent pi-model*) or lumped parameter models (*nominal pi-model*), (ii) frequency-dependent and frequency-independent models and (iii) offers the possibility to model multiple parallel circuits, with or without mutual impedances.

SinCal offers lumped (*nominal pi*) and distributed parameter (*equivalent pi*) models. The inputs may be given as frequency-independent zero-sequence and positive-sequence series impedances and shunt admittances.

3.1.3 Cables

The series impedance and shunt admittance of cables are calculated by cable constants routines using the cable cross-section, cable laying configuration and material parameters of the conductors, insulators and the earth [3].

Cables can be single-core or multi-core, and can be buried directly underground or pipe-type enclosed.

Modeling Guidelines

Transmission line model In frequency domain studies, frequency-dependent models should always be preferred whenever data is easily available. In remote parts of the system, or at voltage levels lower than the one of interest, a nominal PI model may also provide sufficient accuracy [15, 40].

Skin Effect As for overhead lines, skin effect should be modeled for harmonic studies. Skin effect can be included by equations based on Bessel functions [33].

Proximity Effect Proximity effect should be considered only when cable conductors are in close proximity, e.g., in multi-core cables or in cables which are buried with short inter-core distances. Both proximity and skin effect can be critically important since they can lead to large reduction in resonant peaks [41].

Cable Design Characteristics The cable geometry and material parameters of the conducting and insulating layers should be represented as detailed as possible. As the models may not include all cable characteristics in detail, conversion formulas such as the ones introduced in [33] may be used.

Cable Layout The cable layout, e.g., burial in trefoil or flat formation, should be carefully modeled as it impacts the frequency and magnitude of the resonances, and the number of resonances. It also determines whether the cable system is balanced or not.

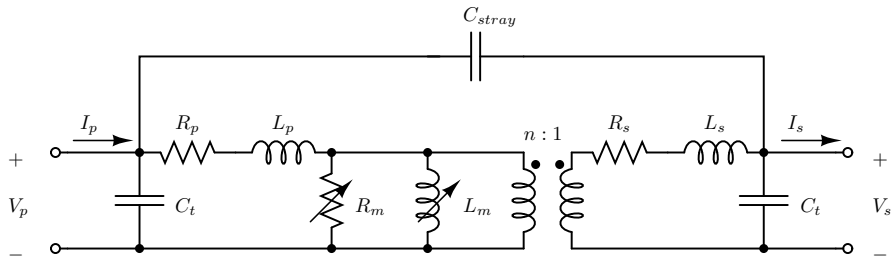

Figure 3.2: Single phase equivalent transformer model (T-model).

Sheath bonding Sheath bonding affects the resonance behavior of the cable and should be modeled in detail. The impedance of the sheath wires may effect the magnitude of the resonance frequencies.

Distributed Parameter Effects As for overhead lines, the cable model should be selected depending on the study requirements. The nominal PI model can be used for shorter cables, while for the cables longer than 2-5 km the distributed parameters model should be used .

Availability in Software

PSCAD offers frequency-dependent cable models (*phase or mode*)) with both pipe-type and coaxial group configurations. It provides a few algorithms with different accuracy levels for performing calculations. It allows for modeling sheath bonding in detail, or to use "ideal" sheath bonding. The latter option is an approximation and may lead to shifts in the resonance behavior of the cable. It should be noted that the phase model should always be preferred over the mode model, due to the significant frequency-dependency of the transformation matrices.

DigSilent PowerFactory offers a frequency-dependent cable model (*equivalent pi*) with up to three single core cables (each up to three conducting layers). Cables can be modeled as directly buried or as pipe-type cables.

It supports calculations of the cable parameters using modified Bessel functions. The ULM model of the cable is fitted before performing the EMT simulation. Supported are procedures for the estimation of the characteristic impedance Z_c approximation. The propagation function can be fitted approximately or using modal-domain or phase-domain fitting.

SinCal offers lumped (*nominal pi*) and distributed (*equivalent pi*) parameter models. The inputs may be given as frequency-independent zero-sequence and positive-sequence series impedances and shunt admittances.

3.2 Transformers

3.2.1 Model Types

Transformers are modeled in several ways. The ones described here are the classical, simplified and Unified Magnetic Equivalent Circuit (UMEC) model [12, 29].

Classical Model

The classical model of a transformer employs ideal transformer or its T-transformer representation. Depending on the core and winding design, the current-flux dependence of the core exhibits saturation effect. Saturation in the case of classical transformer representation is modeled either as a varying inductance across the winding, or with a compensating current source across the winding closer to the core [29].

The commonly used model suggested in CIGRE brochure [23] is depicted in Fig. 3.2. The transformer from Fig. 3.2 represents single phase two-winding transformer model. The same model is considered in the various publications of the interest [12, 32].

Simplified Model

The common simplified transformer representations consist of the series transformer equivalent, which is defined using rated power, leakage inductance and losses. Fig. 3.3 shows the two most commonly used models.

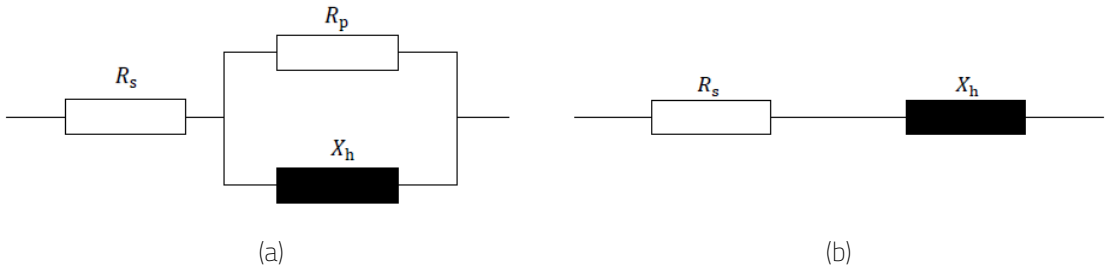

Figure 3.3: Common power transformer models: (a) from [42, 23]; (b) from [44, 43, 45].

Resistance R_s is a series resistance, X_h is determined as a frequency dependent under assumption that leakage inductance L_σ is constant over the range of frequencies [42, 43, 44]:

$$X_h = 2\pi h f_n L_\sigma. \tag{3.9}$$

The resistance is modeled differently depending on the recommended literature. Work [42] suggests $R_s = \frac{X_h}{h\tan(\phi)}$, $R_p = 10\frac{X_h}{h}\tan(\phi)$ and $\phi = \exp(0.693 + 0.796\ln S_r - 0.0421(\ln S_r)^2)$. A DC resistance is necessary for the model in [44], where $R_s = R_{DC}\,(1 + Ah^B)$m, with recommended values $A = 0.1$ and $B = 1.5$. The model from [2] takes short circuit resistance R_t and accounts for the skin effect: $R_s = R_t\ (a_0 + a_1 h^b + a_2 h^2)$, for the condition $a_0 + a_1 + a_2 = 1$. All of these models provide high accuracy, taken into account that they are developed for the purpose of modeling a particular transformer, i.e., the validity of these formulas needs to be checked against measurements for each transformer. They show that the reactance can be modeled as linearly increasing with the frequency [23].

This type of model may be expanded to a multi-winding transformer, e.g., a three-winding transformer. As an example, the positive and negative, and zero sequence impedance of an autotransformer with YNa0(d) configuration is shown in Fig 3.4. In Fig. 3.4, H, X and Y refer to the high-voltage, low-voltage and tertiary voltage side respectively. The per unit leakage impedances may be obtained from the per unit leakage impedances Z_{HX}, Z_{HY} and Z_{XY}, as obtained using the short-circuit test, and impedance to ground Z_g as [46]:

$$\begin{bmatrix} Z_X \\ Z_Y \\ Z_H \end{bmatrix} = \frac{1}{2}\begin{bmatrix} 1 & -1 & 1 \\ -1 & 1 & 1 \\ 1 & 1 & -1 \end{bmatrix}\begin{bmatrix} Z_{HX} \\ Z_{HY} \\ Z_{XY} \end{bmatrix}, \text{ and} \tag{3.10}$$

$$\begin{bmatrix} Z_{X0} \\ Z_{Y0} \\ Z_{n0} \end{bmatrix} = \frac{1}{2}\begin{bmatrix} 1 & -1 & 1 & \frac{n-1}{n} \\ 1 & 1 & -1 & -\frac{n-1}{n^2} \\ -1 & 1 & 1 & \frac{1}{n} \end{bmatrix}\begin{bmatrix} Z_{HX} \\ Z_{HY} \\ Z_{XY} \\ 6Z_g \end{bmatrix}, \tag{3.11}$$

where n is the winding transformation ratio. The phase (or physical) domain model may be derived from these sequence impedances using the Fortescue transform.

UMEC Model

UMEC model describes inductive couplings according to physical configuration of the transformer magnetic core [12]. This model is represented with reluctance $\mathscr{R}$, magnetic flux ϕ and magnetomotive force. This model treats core saturation differently using piecewise-linear technique [29].

3.2.2 Modeling Guidelines

Transformer model The simplified model is the model of choice for the resonance analyses in [23]. More elaborate models, e.g., the one introduced in [12], may be used when the frequency of interest shifts towards a higher frequency region.

Transformer stray capacitance The transformer stray capacitances should be included in the studies above $3-4$ kHz [23, 32, 12].

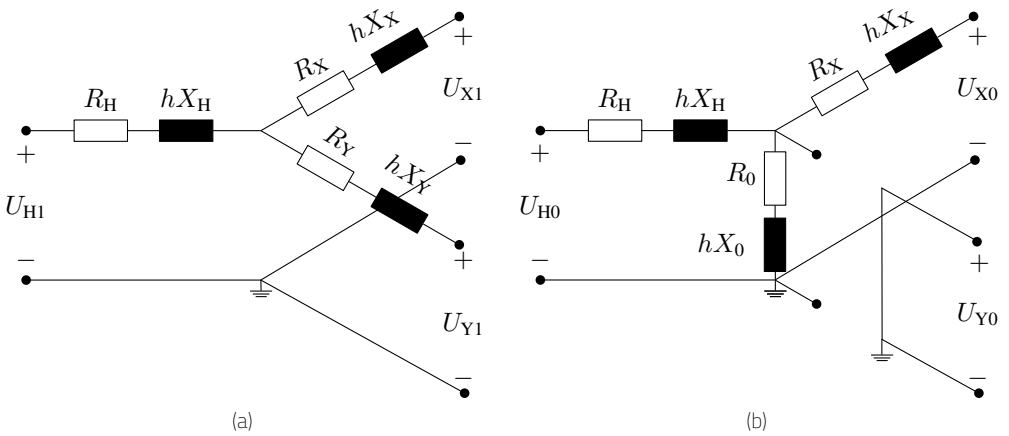

Figure 3.4: Three-winding transformer model for autotransformer with YNa0(d) configuration in positive and negative sequence (a) and zero sequence (b).

Transformer magnetizing impedance The magnetizing impedance (R_m and L_m) can be ignored in the normal conditions. However, if the saturation of the transformer becomes of the primary interest, then the effect can be captured using current source in the place of R_m and L_m, which should be carefully designed from the current-flux curve [23]. IEEE std. 519 [20] says that if the transformer is not a significant source of harmonics, the magnetizing impedance can be neglected.

Transformer tap position The tap position affects the leakage reactance and the transfer impedance to the other side of the transformer. The leakage resistance variation can produce the phase shifts in resonant frequency. It is recommended to capture the tap changes in the harmonic studies [23].

Transformer Losses There are two major resistances: losses inside the conductor (C_u core losses) and losses inside magnetic core (F_e-loss resistance). Although the transformer's resistance varies with the frequency, formulas to take this into account should not be applied without verification against transformer measurements [21]. In case no measurements are available, the resistance at power-frequency can be used first. In a second step, the sensitivity of the resonance towards transformer resistance can be analyzed by calculating the harmonic resonances using a frequency-dependent resistance according to one of the formulas introduced in [21]. Temperature variation has an impact on the resistance of the transformer. However, this impact is estimated as low and thus, less concern in the modeling [21].

Transformer Vector Group The vector group of the transformer windings influences the resonance behavior and should be taken into account in the model.

3.2.3 Models in Commercial Software

PSCAD

PSCAD supports both *classical* and *UMEC* transformer model with different winding configurations and saturation models. Frequency-dependency of the parameters is not considered. In the standard auto-transformer model, copper losses are not included. Stray capacitances are not supported in the standard models.

DigSilent PowerFactory

Transformers are modeled as the *classical* T-equivalent circuit for the positive and zero sequence from the vector group, transformer ratio and the quantities computed from the open-circuit and short-circuit measurements [47]. Stray capacitances as shown in Fig. 3.2 can be added, as well as a frequency-dependent zero sequence impedance. Three-winding transformers are also supported.

SinCal

In SinCal, two-winding transformers are modeled as pi-equivalent networks, where the series impedance is the short-circuit impedance and the no-load losses are distributed over the shunt admittances. Frequency-dependency of the parameters can be included, e.g., according to CIGRE models described in [42]. Three-winding transformers are also supported.

3.3 Synchronous Machines

3.3.1 Model Types

In general, the literature indicates that synchronous machines should be modeled by a series circuit of a resistance and reactance, adjusted to the harmonic order h (or n).

In [42], it is recommended to model the synchronous machines by their subtransient reactance $X"_d$ and a series resistance R_1 equal to $0.1X'_{d'}$. The reactance and resistances increase with the harmonic order n as:

$$X(n) = nX"_d \tag{3.12}$$

$$R(n) = \sqrt{n}R_1. \tag{3.13}$$

These equations should be applied with care, as this model may not always be applicable, as shown on p 2-32 in [21]. Especially with respect to the resistance, the model may become very inaccurate.

In [20, 48], it is recommended to represent machines by a reactance which is equal to half the sum of the subtransient reactance of the direct- and quadrature axis or the negative sequence reactance. The harmonic impedance increases with the harmonic order:

$$X(n) = nX_2, \text{ or} \tag{3.14}$$

$$X(n) = n\frac{X"_d + X"_q}{2}, \tag{3.15}$$

Alternative approaches have been suggested, e.g., to use a resistance variation proportional to n^{α}, with α in the range of 0.5-1.5 [49].

3.3.2 Modeling Guidelines

Model Type The synchronous machine may be represented by a series of a resistance and a reactance.

Reactances IEEE Std 519-1992 [20] recommends to model machines by their subtransient reactances, taking the average of the direct and quadrature axis. Reactances should be modeled by the order of the harmonic frequencies. This is repeated in IEEE Std 3002-2018 [48], where also the resistance according to (3.13) is recommended.

Frequency-dependency of resistance With respect to frequency variation, brochure [21] recommends asking manufacturers for detailed information whenever a large generator is close to the point of interest. Although the modeling method for frequency dependency of the parameters stated above is a simplification, it is widely accepted due to sparsely available machine data and difficulties to include more detailed models in existing software.

3.3.3 Models in Commercial Software

DigSilent PowerFactory

DigSilent PowerFactory offers the synchronous machine model ElmSym, in which the machine is represented by a reactance and a resistance. In a frequency sweep, it is represented by an impedance model with frequency-dependent impedance characteristics. The inductance at fundamental frequency is calculated as the average of the d and q components of the subtransient inductance. The inductance changes with the harmonic order as in (3.12). Furthermore, a frequency-dependent characteristic may be given to the inductance and resistance.

PSCAD

The synchronous machine model incorporates mechanical as well as electrical parts. It does not offer frequency-dependency of its electrical circuit parameters.

SinCal

For SinCal, there was no description of a standard model for synchronous machines.

3.4 Shunt Compensation - Reactors

Reactors are used to absorb the excess reactive power, e.g., generated by cables.

In [21], it is recommended to collect detailed data for those shunt elements in the network that are relevant to the study (especially those connected close to the point of interest. In this respect, inrush/outrush current limiters of capacitor banks (if any) may be important to model, as well as the resistive losses of any shunt reactors in the model.

3.4.1 Model Types

Saturable Inductor With Fixed Losses

In [50], shunt reactors have been modeled as a saturable inductor with a parallel and series resistance (with a fixed value) representing iron and copper losses, respectively. It should be noted that in a frequency assessment, saturation cannot be included given that this leads to non-linear behavior.

Equivalent circuit with Inductances, Resistances and Capacitances

In [12], an equivalent circuit diagram with inductances and resistances, and inter-layer and layer cross-over capacitances is proposed. The model without capacitances (purely inductive) was found to be accurate until 3 kHz, whereas the model with capacitances is accurate until 10 kHz. Frequency-dependence of the resistance was not included, and the models were found to provide slightly less damping compared to the measurement results [12].

3.4.2 Modeling Guidelines

Model Type In the simplest case, shunt reactors can be represented by their inductance. In case of reactors close to the point of interest, losses can be represented by a resistance put in series with the inductance.

Capacitive effects In the low frequency range (e.g., < 3 kHz according to [12]), reactors can be modeled as an inductive element, whereas in the high-frequency range, capacitive effects must be considered. If auxiliary elements are present, these should be modeled as well. In [39], it is stated that shunt reactors behave as inductors within the frequency ranges for TOV, and that capacitances do not need to be considered. It is also stated that saturation of the magnetization inductance, residual flux and losses play an important role in the generation and damping of temporary overvoltages.

Resistive losses Losses should be included if data is available, albeit that at low frequencies a single-frequency model may be sufficient. With respect to the resistive losses, [6] states that these have only a minor impact on resonances but have a significant effect during cable energization, discharge and zero-miss.

3.4.3 Models in Commercial Software

DigSilent PowerFactory

The Shunt element (ElmShunt) in DigSilent PowerFactory offers the possibility to model an RL, RC or RLC-shunt. The element can be configured in various ways (connections). For harmonic analysis, a frequency-dependent characteristic may be given to the RLC parameters. The Shunt element does not take into account capacitances except for a capacitance to ground in certain configurations.

PSCAD

Besides basic components (such as inductors and resistances), a model for a shunt device is not available in the PSCAD library and should be user-created.

SinCal

Shunt reactors can be modeled in SinCal using Inductive Shunt Branches.

3.5 Passive Loads

Loads play an important role within harmonic analysis. Depending on their type, they may (e.g., resistive loads) or may not (e.g., inductive loads) provide damping for a certain harmonic frequency. CIGRE WG B4.47 [21] claims that although data on loads may be difficult to obtain, it is incorrect to assume that, in the absence of load data, a conservative or safe assessment of network harmonics is done. When neglecting load, the damping may decrease as expected, but the network resonant frequencies especially of low order harmonics may shift as well. IEEE Std. 519 [20] describes the load model as one of the most important elements in the transmission system representation.

Although loads play an important role, the literature in general points out that there is no "universal and generic harmonic load model" [21, 42, 45]. Two points which pose particular challenges for modeling the load are:

1. The extent of modeling detail with respect to voltage levels below the voltage level of the system under study will determine what is considered as "load" and hence also the load model. If a substantial part of the "lower-level" network is modeled, for a harmonic impedance study of the EHV network, "the frequency response at a given bus is not significantly affected by the model of the loads at lower voltage levels" [40].

2. The rationale behind several load models from older sources has been lost over time, making that it is not possible to verify the correctness of these [21].

According to CIGRE TB 766, loads are categorized into linear loads and non-linear loads. The linear loads consist of a static part and a rotating part. The static part can be modeled fairly accurate according to parameters calculated at fundamental frequency, whereas the rotating parts cannot. Nonlinear loads are often associated with power-electronic loads, and the brochure mentions challenges to model these correctly.

In transmission studies, loads may be aggregated according to a bottom-up approach or a top-down approach. In the bottom-up approach, an aggregate model is the result of lumping together detailed component models. In the top-down approach, a load model is derived based on its behavior, e.g., through measurements.

The aim of this section is not to provide an exhaustive overview of harmonic load models, but rather point out options in the literature and the implications they have. A detailed comparison of load models is given in CIGRE TB 766 [23].

3.5.1 Model Types

The types of load model depends on the transmission level at which the load is modeled: EHV, HV, MV or LV.

Low-level Linear Harmonic Models

Low-level linear harmonic load models typically consists of an arrangement of resistances and reactances to model the static and rotating part of the load. A review of the load models considered over time by CIGRE and IEEE is given in CIGRE TB 766 [23]. In general, the static part is modeled by a parallel or series RX-circuit, where the circuit parameters are determined based on the fundamental frequency power flow. The rotating part is also modeled using a parallel or series RX-circuit, where the parameters are usually frequency dependent. For the rotating part, it is recommended not to use parameters based on the fundamental frequency power flow, but using a subtransient reactance and a resistive equivalent using its losses [21]. Several (empirical) formulae for the R and X part have been posed also based on measurements, but the rationale behind these may have been lost over time [21].

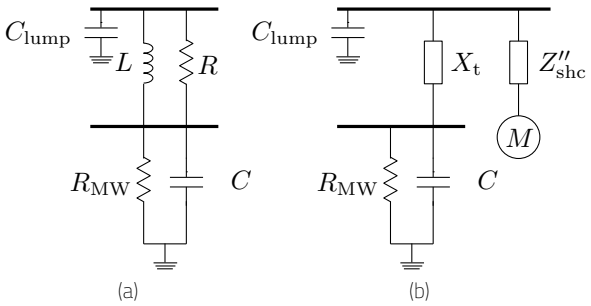

Figure 3.5: Lumped Equivalent Load Network of National Grid (a) and Scottish Power (b) [21]

Load modeling comparisons in the literature

In a first approach [51], the load at the transmission level is modeled as an equivalent RL or RC circuit, placed at the secondary side of the transformers between the primary network (network under study) and the secondary network (lower voltage levels). The parameters for the RL- or RC-circuit are obtained from a loadflow at the secondary side of the transformer. The parameters are frequency-independent.

In [47] and [51], the harmonic impedances seen at the primary and secondary side are compared for a simplified circuit and a full circuit. The comparison shows that:

- The simplified equivalent circuits produce more damping at the first resonance peak compared to detailed modeling at the secondary side.
- A frequency shift is observed at the first resonance peak.
- For larger frequencies, larger differences are observed, e.g., some resonance peaks are not present for the simplified circuit.

[6] discusses that a series RL circuit provides less damping compared to a parallel RL circuit, and hence may lead to a more conservative assessment.

Lumped Equivalent Load Networks

In [21, 23], two transmission level aggregated equivalent load networks as used by National Grid and Scottish Power are introduced for a harmonic load analysis (Fig. 3.5). In Fig. 3.5, the model includes a lumped capacitance (C_{cap}), representing the total cable capacitance at bus L1, a lumped transformer reactance along with a damping resistance R, representing all transformers connected between L1 and the LV system and the customers connected at LV. The LV bus is represented by a resistive load and a capacitance to represent PF correction. . Motors can be put in parallel with the resistive loads, and are modeled using a series impedance of its subtransient reactance and a resistance equivalent to its losses. The model by Scottish Power is similar to the one by National Grid, but parameters are calculated in a different manner. It is important to note that all parameters depend on the load composition, level of load and distribution system parameters.

3.5.2 Modeling Guidelines

Loads are said to have an important damping effect, even at low load levels. In [21, 23], it is found that neglecting load may lead to over-conservative results.

Based on the literature, following guidelines are compiled:

1. Based on the literature, at least the primary system should be modeled in complete detail, and attention should be paid to the secondary system. The type of transmission lines in the secondary system was found to have an influence on the resonance peaks [51].
2. Equivalent loads placed at the secondary of the downstream network: RL-circuits of different types in general lead to similar results, whereas a lumped equivalent load network shows more resonant peaks as in this case, capacitances are also modeled [23]. However, in the latter case, the occurrence of these resonance peaks should be verified by measurements.
3. Equivalent circuits placed two networks downstream: the load equivalent does not have a significant influence on the resonance peaks observed in the primary system [23].

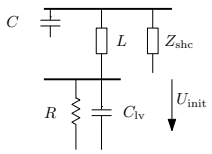

Figure 3.6: Load Impedance 2 model in DigSilent

4. If detailed and accurate information on the load composition is available, we recommend to model these in detail.
5. Using RL or RC circuits directly attached to the secondary of the transformers connected to the primary system (e.g., when speeding up simulations), may provide satisfactory results in a first assessment, but should be used with care, as damping may be overestimated, resonance frequencies may have shifted and certain resonance peaks may not be seen [15].

3.5.3 Models in Commercial Software

DigSilent PowerFactory

In DigSilent PowerFactory, models for a "General Load", "Complex Load", "Medium Voltage Load", "Low Voltage Load" and "Partial Load" are available.

The "General Load Model" comes in three different options:

- The impedance Model 1 can model loads as a series connection of an inductance and resistance or as a parallel connection of an inductance and a capacitance. The RL or RC parameters are frequency independent and calculated from a preceding load flow.
- The impedance Model 2 models loads in a similar structure as the SP lumped equivalent load network (Fig. 3.6). The transformer is modeled by its leakage resistance only.
- The current source model models the load as a constant current source, for which the currents are calculated based on a load flow.

The "Complex Load Model" is a combination of a static load and an induction motor. The static part is a parallel RX-circuit with voltage dependent parameters. The dynamic part is a simplified asynchronous motor model. For this type, the parameters may be frequency-dependent.

The "Medium Voltage Load" is an impedance model behind a transformer. The transformer is modeled by its series impedance. The load is an series RL, parallel RC or combined RL circuit with a parallel capacitor.

The "Low Voltage Load" is represented as an RX-equivalent circuit, impedance which is either inductive or capacitive. The inductive circuit is a series circuit, whereas the capacitive circuit is a parallel circuit.

PSCAD

PSCAD offers the possibility to implement loads as (i) a combination of standard R, L and C components, (ii) a "fixed load" model and (iii) a frequency-dependent network equivalent.

In a harmonic analysis, the "fixed load" model is represented by a parallel RL or RC-circuit calculated at the fundamental frequency. The "fixed load" model in PSCAD is offered as a voltage and frequency-dependent load model, having P and Q in the form of

$$P = P_0 \left(\frac{V}{V_0}^{NP} \right) (1 + K_{PF} dF) \tag{3.16}$$

$$Q = Q_0 \left(\frac{V}{V_0}^{NQ} \right) (1 + K_{QF} dF) . \tag{3.17}$$

(3.18)

However, a comparison of a frequency scan of a load model with a frequency scan of an RL-circuit with R and L calculated at fundamental frequency gives the same results.

The frequency dependent network equivalent component is a multi-port component which may represent an equivalent load circuit as described above. The component approximates the input parameters with rational function, using Vector Fitting. The input parameters may be given in many forms, including a frequency scan or network parameters (e.g., impedance, admittance, scattering).

SinCal

SinCal offers the possibility to include the CIGRE WG 36.05 load model with the parallel RX and X branch (France EDF model).

3.6 Frequency-Dependent Resistance

Skin-effect causes the resistance of several components (transformers, generators, shunt reactors) to change with frequency. In the literature, various approaches have been proposed. A common approach is to use [21]:

$$R_h = R_0 n^{\alpha}, \tag{3.19}$$

in which R_h and R_0 are the resistance at order n and 0, and α depends on the network component to be modeled (e.g., 0.5-1.5 for the synchronous generator model).

Alternative approaches have been suggested, as (3.19) may overestimate damping at low orders and underestimate damping at high orders [21]. It should be noted that all approaches should be applied only within the frequency range for which they are valid.

3.6.1 Models in Commercial Software

DigSilent PowerFactory

DigSilent PowerFactory offers the use of three methods for including frequency-dependency of resistance (or even inductance and capacitance). Either a polynomial (ChaPol) or a user-defined table (TriFreq and ChaVec) may be used.

The polynomial characteristic $y(f_h)$ is a multiplicator for the fundamental frequency resistance:

$$y(f_h) = (1 - a) + a\left(\frac{f_h}{f_1}\right)^b, \tag{3.20}$$

in which f_h and f_1 are the harmonic and fundamental frequency, respectively, and a and b are user-definable.

The frequency-dependent characteristic may be applied to, e.g., line elements, machine elements (Synchronous, Asynchronous), shunt filters, voltage sources, complex load, transformer elements.

PSCAD

PSCAD does not seem to offer standard routines for including frequency-dependent resistances, except for the frequency-dependent network equivalent.

SinCal

SinCal offers four options for setting frequency-dependent behavior; (i) no frequency dependency, (ii) R constant, (iii) X/R constant and (iv) impedance characteristics.

3.7 Active Components (Power-Electronic)

According to [23], the recent proliferation of converter-based devices implies the need to account for both harmonic emissions and harmonic impedances when modeling active components for harmonic or resonance studies. The generic model structures are the Thévenin or Norton equivalent circuits. Consequently, these models consist of a **harmonic voltage or current source** and of a **harmonic impedance or admittance**. It should be noted that these representations have limitations as they are linear representations of devices which normally present a nonlinear behavior and whose characteristic may actively change with the level of harmonics. In particular, active components introduce couplings that may require representation by the equivalent circuit:

- The coupling between sequences can be represented by means of an impedance/admittance matrix with sequence coupling terms;
- The coupling between components of different frequencies can be represented by a harmonic domain model.

The resulting harmonic impedance/admittance should account for both:

- the passive elements that connect the active component to its network (LCL filter, power transformer, etc.);
- the control loops (inner control loops, outer control loops, active filter, etc.).

Both aspects influence the harmonic behaviour of the component. It is also mentioned in [23] that further work will be required to develop robust methods to adapt the frequency domain harmonic model to the selected control strategy and to the operating point of the component.

Converter-based Wind Generation

The above considerations hold for the modeling of converter-based wind generation. Converter harmonic impedance and filters should be included when modeling type 3 and type 4 WTGs. Therefore, the use of Thévenin/Norton equivalents is recommended instead of the constant current source approach. Detailed WTG models capturing these elements should be requested from vendors to improve accuracy in harmonic studies involving wind farms.

The harmonic emission profile of WTGs is a function of the operating point. The worst-case operating point at each harmonic order is often used to yield a conservative result, although it is also possible to implement look-up tables to represent the harmonic behaviour at different operating points.

The equivalent harmonic impedance is the total converter output impedance which should include the impact of closed-loop controls. Any other passive component (such as the main reactor impedance, passive filters and turbine transformers) must be captured either as part of the equivalent harmonic impedance or explicitly as an external component.

HVDC Converters

Line Commutated Converter (LCC) In the first instance, LCC HVDC converters are often regarded as harmonic current sources, for which the harmonic current emission does not vary with the AC side impedance. Although this simplification gives approximately correct results at high harmonic orders, it can be unsatisfactory for low orders, particularly for the 3rd harmonic. Therefore, a more complete model is necessary for such low order harmonics:

Reactive power compensation devices (switchable filters and/or capacitors) must be modeled as they will interact with the harmonic impedance of the grid. It is recommended to analyse a range of operating points and status of filters and capacitor banks to ensure that they do not introduce excessive resonances or harmonic distortion in the grid.

Voltage Source Converter (VSC) As the harmonic generation of VSC HVDC stations is typically very low, it is normally sufficient to calculate a non-consistent set of maximum harmonic voltages over the complete range of operation of the converter, and use this as the modeled harmonic generation, represented as a voltage source behind the converter internal harmonic impedance.

The converter harmonic impedance must include the passive components (power transformer and any filtering) as well as the internal impedance of the converter.

Flexible AC Transmission System

Flexible AC Transmission System (FACTS) devices generate harmonics depending on their configuration, control strategy and switching scheme. They must be adequately modeled for harmonic/resonance studies. Modeling recommendations are discussed below for Static Var Compensators (SVCs) and STATCOMs, which are the two most common LCC-based and VSC-based FACTS devices.

Static Var Compensators In practice, SVC configurations vary from one project to the next, but may generally contain a thyristor-controlled reactor (TCR), a thyristor-switched capacitor (TSC), LV and/or HV AC filters and a transformer. The harmonic emission spectrum of SVCs is related to thyristor-based converter topology. In this technology, harmonics are generated due to the non-linear nature of the thyristor switches. Moreover, the harmonic emission spectrum depends on the operating point of the device.

Modeling recommendations are to represent the TCR as a harmonic current source with its harmonic impedance, while the other components are represented by their harmonic impedance. To account for the dependency on the operating point of the device, the harmonic source emissions and the harmonic impedances must be determined for all possible configurations of the SVC (with the TSC on or off, with different firing angles, etc.).

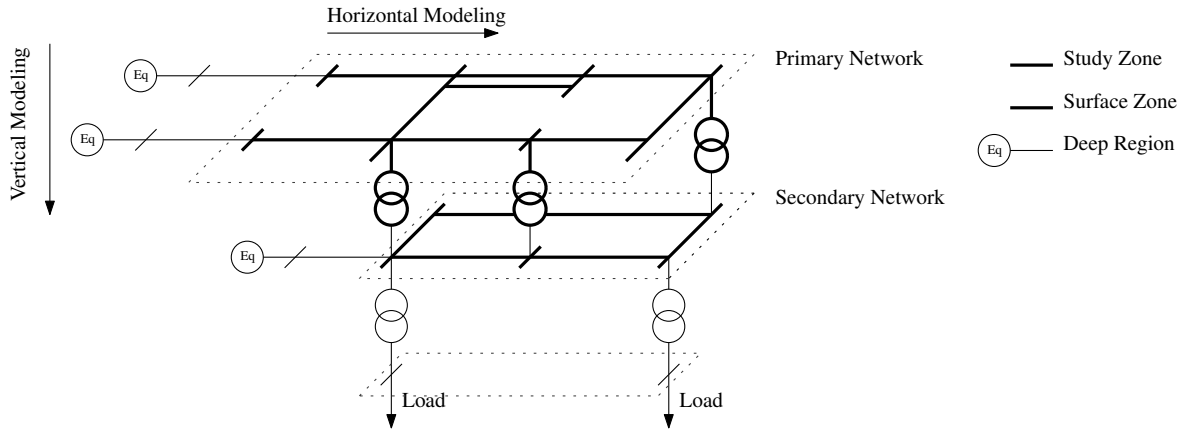

Figure 3.7: Network modeling level detail

STATCOMs The harmonics generated by STATCOMs are typically of very low magnitude. They depend on the operating point and are project/solution specific.

Modeling recommendations are to represent the STATCOM by means of an active harmonic voltage source behind the converter internal harmonic impedance. Given the low magnitude of the generated harmonics, it is normally sufficient to calculate a non-consistent set of maximum harmonic voltages over the complete range of operation of the converter.

The harmonic impedance model must include not only the passive components of the STATCOM (e.g. harmonic filter, series reactor, step-up transformer) but also the VSC internal impedance defined by the operational mode, the controller transfer functions and its corresponding parameters. The harmonic impedance is operating-point dependent in the low frequency range (within the bandwidth of the converter inner current control loop).

3.8 Network Modeling Detail and Network Equivalents

There are not a lot of general rules to define the extent of the network that is to be modeled in detail, and network reduction mainly comes from engineering judgement. According to [23], full-scale system models in frequency domain are used by the French, Danish, Irish and British TSOs for their harmonic studies. To partition the network into a main study system and external interconnected systems, sensitivity methods described in [52] can be employed as an analytical tool. Such sensitivity studies are also recommended in [22], which suggests to perform such studies by progressively extending the horizontal and vertical distance (see Fig. 3.7) of the detailed modeling until the frequency response of the network (e.g. of the driving-poin impedance at the point of interest) does not change in a significant manner, while giving priority to electrical components with high capacitive parts, e.g. cables.

Two possibilities exist to approach network modeling [15]:

1. Top-down approach: In this approach, a detailed reference network is modeled first. Reduced networks are constructed based on simplifications in the reference network and their accuracy is validated against the reference network.

2. Bottom-up approach: In this approach, a small portion of the network to be investigated is first modeled (e.g., up to two or three buses from the point of interest). Then, model detail is added until certain performance criteria (e.g. the impedance spectrum) do no longer change significantly.

3.8.1 Network Level Detail on the Same Voltage Level

For high-voltage levels, the existing literature recommends to model accurately at least the entire primary network [45]. The level of detail of components in fact depends on: (i) relative position of component with respect to the bus of interest and (ii) relative sizes of the components [45]. The recommendation of accurately representing the primary network stems from the low electrical distances found at high voltage levels. A study done by RTE [10] confirms this, as only the complete model of the 400 kV model provided the most accurate results. Other studies conducted in EMTP-RV by the French TSO RTE on a full-scale model of the French transmission system show that using reduced models that model the network up to 1, 2 or 3 nodes away from the study points result in significant changes both in the magnitude and frequency of resonances [53].

To determine model detail, the system is typically split into three zones: a study zone (zone (i)), a surface zone (zone (ii)) and a deep region (zone (iii)). In the study zone, the transmission lines should be represented using the most accurate models (including frequency-dependency of parameters, detailed representation of cross-bonding of cables,...). In the surface zone, the transmission lines may be modeled using simplified approaches, such as Bergeron models or nominal PI sections. The deep region is modeled by a 50 Hz equivalent circuit based on the short-circuit strength of the external grid at that point. The rationale behind this is that high-frequency phenomena exhibit a higher attenuation compared to low-frequency phenomena. In [23], it is stated that an external network (deep region) should be represented as a power frequency network equivalent only if it has no resonances within the frequency range of interest, or if it is so far away that it does not impact the frequency response at the buses of interest.

The boundary between the three zones is not clearly defined and is typically done empirically on a case by case basis. As implemented by the Spanish and French TSO's in [40] and [54], the frequency-dependent network equivalent can be obtained by first extending the network horizontally starting from the highest voltage level, and then extending the network vertically to lower voltage levels until the network impedance does not show a significant change [23]. Applications of this approach indicate that the study zone may extend up to 7 layers in the primary network [40]. An application of this principle in [15] indicates that the zone (i) extends up to three buses from the point of interest (i.e., the line to be studied), whereas zones (ii) and (iii) may start from two to three buses from the point of interest.

3.8.2 Frequency-Dependent Network Equivalents

Resonance Analysis

A frequency dependent network equivalent should be used whenever the (modeled) network (i) has a resonance within the frequency range of interest or (ii) if it is close to the bus of interest [23]. Moreover, the frequency dependent network equivalent should represent all changes in its frequency response, e.g., due to topological changes in the external network.

Background Harmonic Amplification

To avoid calculating the harmonic impedance of interest for all possible external network impedances, a common practice is to consider only certain external network impedances based on an envelope of these external network impedances constructed in a R-X diagram. The latter diagram visualizes the external network harmonic impedances as a function of harmonic order in the R-X plane. The harmonic impedances can be grouped together into envelopes (which may be different for different harmonic orders), as to determine the boundary values for the network impedances to be considered. Although according to [21], each network should be studied on a case-by-case basis, some guidelines are given to reduce the number of calculations.

For instance, in [7], the 400 kV network is represented by a Thévenin harmonic impedance which is determined based on a detailed representation of that network. As the harmonic impedance changes with changing network conditions, a large number of harmonic impedances was considered.

The discrete points on an impedance polygon only represent the harmonic impedance of the network at one harmonic frequency, and therefore they should be used only for calculation of harmonic impedances at the frequency at which they are evaluated.

3.8.3 Network Level Detail Across Voltage Levels

The literature divides the network under study between the 'primary network' and the 'secondary network' [42]. The primary network is that part of the network which is at the same voltage level as the phenomenon/component under study. The secondary network contains all other parts of the power system. As an example, for an EHV study at 380 kV, the primary network is the EHV at 380 kV and the secondary network consists of all lower levels.

The existing literature recommends to investigate which part of the secondary network to model in detail [42]. In [45], it is strongly recommended to model at least part of the secondary network and put load models there. In [51], it was observed that putting loads directly at the secondary of the transformers in the primary network causes slight shifts in the resonance frequencies and provides increased damping.

3.8.4 Modeling Guidelines

1. A top-down modeling approach may be used when detailed information is available for all components of the network, and a reference network which is to be reduced can be constructed. A bottom-up approach

may be used when this information is not available, and constructs a reduced network starting from the point-of-interest.

2. The extent of the network to model in detail must be assessed on a case-by-case basis. The network model can be divided into three zones with varying levels of model detail, which are the study zone (e.g., most detailed transmission line models), surface zone (e.g., less detailed transmission line models) and deep region (50 Hz network equivalents).

3. The 50 Hz network equivalents may be used whenever (i) the external network has no resonances within the frequency range of interest and (ii) the external network is sufficiently far from the point of interest.

4. An external network not meeting the above requirements should not be represented by a 50 Hz equivalent, but should be represented by a frequency-dependent network equivalent or harmonic impedance. This frequency dependent network or harmonic impedance should moreover reflect different operating scenarios (or at least the worst case scenarios). For the worst case scenarios, polygon envelopes may be constructed in the R-X diagram and discrete points for each harmonic may be taken (taking into account that the outcomes of the study are then only valid at the frequency of the polygon envelope).

5. The extent of the network to be modeled across voltage levels should be assessed on a case-by-case basis. As concluded in Section 3.5, modeling part of the network at lower level and attaching loads there provides more accurate results in comparison to modeling loads directly at the secondary of the transformers connected to the primary system. In a first assessment however, loads may be modeled as parallel RL- or RC-circuits obtained from a power flow study [15].

3.8.5 Models in Commercial Software

DigSilent PowerFactory

The external grid model can be used to model the grid at the point beyond the nominal network. The external grid model is represented by an RL-impedance, which may take frequency dependent parameters. The frequency dependency of the parameters can be described by a polynomial or a vector (to take into account skin effect) [DigSilent Manual p. 820].

The network reduction tool offered in DigSilent PowerFactory is only suitable for load flow or short-circuit calculations. In the former, it keeps the sensitivities.

PSCAD

PSCAD offers a frequency-dependent network equivalent, as mentioned in Section 3.5.3. The frequency-dependent network equivalent calculates the equivalent impedance seen from that bus and fits it using Vector Fitting techniques.

SinCal

SinCal offers the "Harmonics Resonance Network" component, which calculates the network impedance at any frequency. SinCal takes as input an impedance area in the R-X plane and automatically calculates the minimum and maximum impedance based on this area.

3.9 Summary

This chapter gives an overview of the modeling rules available in the existing literature. Modeling guidelines for components have been summarized in Table 3.1. In accordance with the project scope, emphasis has been put mostly on the passive elements, and first references on power-electronic component modeling have been introduced.

In the chapter, the existing practice for selecting the extent of network to be modeled in detail has been introduced. It was found that such a modeling exercise should be done on a case-by-case basis and that models should be verified using measurements. More details on actual development and full validation of a network model for resonance studies are out of scope of this report.

[1] Simplification to be verified by sensitivity study

Table 3.1: Recommended model types for frequency domain studies

Component	Recommended model type	Alternatives[1]	Section
Overhead Line	Frequency-dependent model (Equiv. PI or ULM)	Nominal PI (only for remote lines or lines at lower voltage levels)	3.1.2
Cable	Frequency-dependent model (Equiv. PI or ULM)	Nominal PI (only for remote lines or lines at lower voltage levels)	3.1.3
Transformer	Simplified model	Classical model (for f>2-3 kHz)	
		Frequency dependent resistance (if data available)	3.2.2
Synchronous Generator	Series RL circuit, R freq. dep., L based on dq-reactances	R freq. independent for first assessment	3.3.2
Shunt reactor	Series RL circuit	L (if no data available on losses or remote element)	3.4.2
Passive Loads	Parallel RX-circuits, split between static and rotating part	Loads as RX circuits based on power-flow at transformer secondary	3.5.2
Active Components (LCC-type)	Complete model if electrically close (esp. filters)	PQ-load if electrically remote	3.7
Active Components (VSC-type)	Passive components and internal impedance as defined by controls	PQ-load if electrically remote	3.7

4

Result Interpretation

In Chapter 2, different calculation methods to be used in cable resonance studies were introduced. This chapter elaborates on the results that each of these methods provides, the specific interpretation techniques that accompany each calculation method and on when to use which method.

The chapter mainly focuses on the frequency scan and the harmonic resonance mode analysis. A voltage scan or background harmonic amplification calculation are methods derived from the frequency scan.

4.1 Preliminary Analysis

A preliminary analysis method to calculate an approximate frequency at which resonances can occur was introduced in Section 2.1, which makes use of lumped parameters [1, 20]. In [1], the authors suggest that if the approximate frequency calculated using this method —utilizing an inductance derived from the short-circuit power of the connected grid and the total capacitance of the cable— corresponds to a frequency less than the 13^{th} harmonic, more detailed harmonic studies should be conducted.

4.2 Frequency Scan

4.2.1 Theory

The frequency scan method introduced in Section 2.2 calculates the driving-point (diagonal elements of the impedance matrix, or the Thévenin equivalent impedance of the network seen from that bus [48]) and transfer impedances (off-diagonal elements of the impedance matrix) associated with a chosen test bus at every frequency within the frequency range of concern. Using the driving-point and transfer impedances, series and parallel resonances can be identified as follows: Series resonances ($Z = R$ in (1.1)) are characterized by "valleys" in the magnitude response of the impedance, whereas "peaks" in the magnitude response indicate a parallel resonance ($Z = \frac{1}{G}$ in (1.2)), with the phase angle of the impedance being zero for both types of resonances [2]. As demonstrated for a simple circuit containing both series and parallel resonances in [2], a series resonance can

be triggered by an excitation with a voltage source, while a parallel resonance can be triggered by an excitation with a current source. It is also noted that series and parallel resonances are just a naming tag valid for circuits containing a single mode of oscillation. For a simple circuit containing both series and parallel resonances, the application of the frequency scan method is demonstrated in Fig. 4.1 [2]. As explained before, the valley at 3.5 kHz corresponds to a series resonance ($f_{series} = \frac{1}{2\pi\sqrt{L\cdot(C_S+C_P)}}$), and the peak at 5.03 kHz corresponds to a parallel resonance ($f_{parallel} = \frac{1}{2\pi\sqrt{L\cdot C_P}}$).

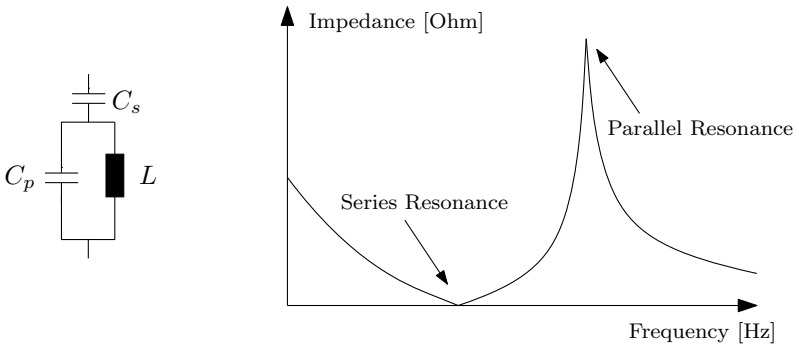

Figure 4.1: Application of the frequency scan method, based on example in [2].

The application of frequency scans during a resonance study is rather straightforward, and gives an indication on the frequency and damping of the resonance peaks, but the results that are obtained from the frequency scan do not give much information about the origin of the resonance, i.e., which equipment is causing or participating in it and which location may be suitable for adding a filter to mitigate it. For TOV studies, the frequency scan may be used to obtain the frequency region of the resonance peak and an indication of the damping at those frequencies. Therefore, for assessing TOV, it is common practice to carry out detailed time-domain simulations following a frequency scan study, focusing on the potential resonance issues in the network that are indicated by the frequency scan, as it was done by EirGrid for the Irish network in [11]. The applications that utilize the frequency scan method are explained in detail in the next section.

4.2.2 Applications in the Literature

- In the temporary overvoltage study analyzing the effect of series and parallel resonances for an increased penetration of cables in the Ireland system reported in [5], frequency scans are performed for different networks to find resonance frequencies under different network operating conditions, before detailed time-domain simulations are run. The results of the frequency scans are also used to determine the most severe switching scenario, by analyzing the frequencies in which a series or parallel resonance occurs, and associating these frequency with a switching event, e.g. choosing transformer inrush as the most severe case when the resonance frequency is close to 100 Hz. In the end, the overvoltages are evaluated based on time-domain simulation results. For more details on this method, see Section 5.

- Frequency scans are used in in [1] for studying the general trends associated with cable resonances. The study considers a cable connected to a grid represented by an equivalent inductance and resistance, representing the grid strength and XR-ratio. In the study, the input impedance (cable input voltage/cable input current), transfer function (cable input vs. cable output current) and output impedance (cable output voltage/cable output current) are calculated. It is concluded that (i) a stronger grid causes a shift of frequency peaks to a higher frequency, but also an increase in magnitude of the peaks, (ii) increasing the cable length lowers the resonance frequency but a decrease in magnitude of the peaks due to the cable resistance, (iii) the sensitivity of the resonance peak magnitudes to the resistive damping is high.

  It is concluded that as the magnitude of the cable transfer function from the sending to the receiving end during resonances is higher for stronger grids, the same harmonic source on the sending end will result in higher harmonic currents at the receiving end for stronger grids.

- In [55], the frequency scan is applied to a simple 10-bus network and the Swiss EHV network in , as part of an undergrounding study of the Swiss power system. The frequency scan results for both networks demonstrate that with the introduction of cables into the system, the resonance frequencies are brought lower.

- In [28], a model of a wind farm connection is made in EMT-type software, which is used to calculate the background harmonic amplification. Time-domain validation of the model against measured switching events show that the model is able to replicate the measured waveforms.

- In [7], problems caused by the 11^{th} and 13^{th} harmonics in the 15 kV system at the Anholt island in Denmark are analyzed by means of harmonic voltage gains, i.e., ratio of the voltages at the 400 kV and 15 kV systems for a specific harmonic frequency. In addition to field measurements to calculate the harmonic voltage gains, frequency scans are conducted to calculate the phase impedances seen from the 400 kV bus, and the harmonic voltage gains from that bus to the 15 kV bus. As a result, the harmonic problems in the 15 kV system were successfully associated with a system resonance in the 400 kV system around the 11^{th} and 13^{th} harmonic, and the calculated voltage gains matched closely to the ones measured in the real system.

- The application of frequency scans in [14] which studies the application of EHV cables in the Dutch network is accompanied by two criteria to interpret the results: the first frequency in which a resonance occurs, and the number of resonance frequencies below 2.5 kHz. As a result of the study, with the introduction of cables, a decrease in the first resonance frequency and a significant increase in the number of resonant frequencies below 2.5 kHz are observed.

4.3 Harmonic Resonance Mode Analysis

4.3.1 Theory

The HRMA first calculates the admittance matrix $\boldsymbol{Y}$ of the overall system at a desired frequency, which is followed by the calculation of its modal decomposition. The diagonal matrix of eigenvalues of $\boldsymbol{Y}$ becomes the main point of the analysis, the inverse of which is defined as the modal impedance matrix. The diagonal elements of the modal impedance matrix are analyzed at the desired frequencies, and possible resonances are detected as peaks in the modal impedances.

The information obtained from the HRMA is especially useful for locating the origin of a resonance and the buses participating in a resonance (e.g., to locate where a filter should be installed to mitigate the resonance). This information is provided by the participation factors, which are related to the eigenvectors of the admittance matrix, which provide an indication of the participation of different buses in a certain mode. By contrast, the magnitude of the modal impedances (i.e., the inverse of the eigenvalues of the admittance matrix) is hard to interpret, in the sense that there is yet no association of the eigenvalue magnitude at the resonance peak to the severity of a resonance. It should be noted that the HRMA only locates parallel resonances[27].

4.3.2 Applications in the Literature

- HRMA has been applied to the German EHV system in [56]. The system under study is composed of 268 nodes, connected only by overhead lines. In the study, only the first 50 harmonic orders are of concern, which is the reason why the authors choose not to model the stray capacitances of the transformers and the frequency-dependency of overhead line parameters. Even though the system does not contain any cables, this application can be used as an example to illustrate how the results of the HRMA can be interpreted. The authors calculate the positive- and zero-sequence modal impedance matrices of the system under study under low (loads having capacitive behavior) and high load (loads having inductive behavior) conditions. As only the resonant frequencies are of concern, the maximum modal impedance at a specific frequency is calculated, and no further analyses regarding individual resonances are conducted. It is observed that the resonance frequencies under both conditions heavily depend on the system operating mode and the switching states of the transmission lines. Moreover, it is found out that the results obtained from the positive- and zero-sequence impedance matrices were different, highlighting the importance of conducting separate resonance studies for positive- and zero-sequence networks of the system. Significant resonances at harmonic orders 23.8 and 45.4 are observed in the positive-sequence impedance matrix during low-load operation. Since the resonance at the harmonic order 23.8 lies between the negative-sequence harmonic order 23 and the zero-sequence harmonic order 24, the authors conclude that a resonance can be triggered if negative-sequence harmonics at the 23^{rd} order are injected. Similarly, the authors claim that the resonance at the harmonic order 45.4 can be excited by a positive-sequence 46^{th} order harmonic. As no significant resonances are observed at the zero-sequence impedance matrix at the harmonic order 24, no possible problems are foreseen.

- In a similar study with the German EHV system, it is shown that as more overhead lines in a section of the studied German EHV system are replaced by underground cables, the number of resonance peaks within the first 25 harmonic orders increase, and a considerable decrease is observed in the magnitude of the maximal modal impedance [57]. When compared to the other applications in the literature, the authors report a similar shift in the resonance frequencies towards lower frequencies, yet as an exception some peaks are observed at higher frequencies with the increase in cables. No analysis is conducted on the magnitudes of the impedances, the nodes participating in the resonance modes or the frequencies at which resonances occur.

- The HRMA is applied to the aforementioned undergrounding study of the Swiss power system in [55], in which the skin effect and the frequency-dependency of the line parameters are explicitly modeled, yet the capacitive and saturation effects of transformers are neglected. Different cases for the replacement of overhead lines with underground cables are studied, and it is shown that when an overhead line that is connected between nodes having a strong participation in the resonance mode is replaced with a cable, a significant drop in the resonance frequency is observed. A similar finding is reported in [58], in which replacement of overhead lines with cables in the IEEE 14-bus test network is studied.

4.4 Comparison of Frequency Scan vs HRMA

To illustrate the conceptual differences between the frequency scan method and the HRMA, their applications on a simple four-bus network are depicted in Fig. 4.2 and Fig. 4.3, respectively. In the frequency scan method, a candidate bus is selected, harmonics are injected at the chosen candidate bus, and the resulting driving-point and transfer impedances are calculated to assess the resonances. In the HRMA, however, the analysis of the impedance/admittance matrix in the modal domain corresponds to the excitation of a specific mode, which can be modeled as a simultaneous injection of harmonics at different buses. The modal impedance for a specific mode is the resulting modal voltage divided by the modal current. The modal voltage is divided over the buses based on the left eigenvector $\boldsymbol{L}$.

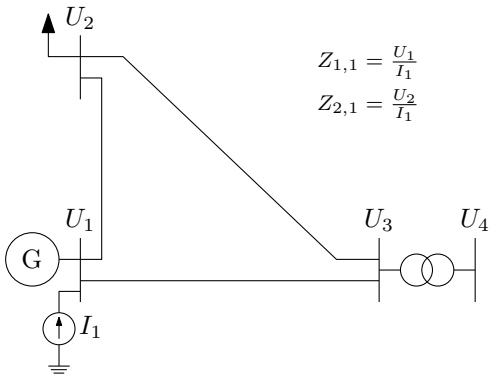

Figure 4.2: Application of the frequency scan method.

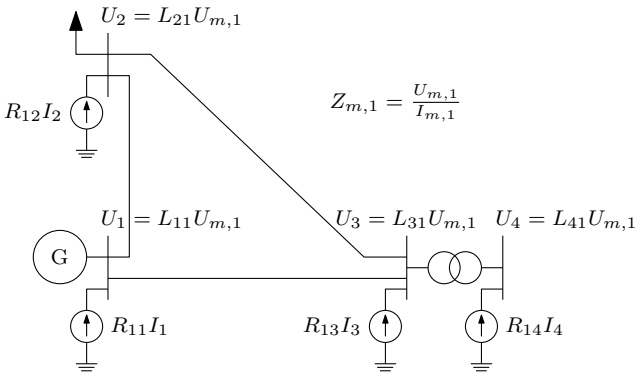

Figure 4.3: Application of the HRMA.

In [27], both the frequency scan and the HRMA methods are applied to two variants of the IEEE 14-bus test system: the original network, and a modified version of the IEEE 14-bus test system, which leaves only one capacitor at bus 9. The frequency scan is carried out by injecting a 1.0 per-unit current at bus 9, which produces the driving-point and transfer impedances of the network at bus 9. Even though the system is modified to contain only one element (capacitor) that can create resonances, it is observed that most of the calculated impedances exhibit resonances, making it harder to identify the participation of the buses in the resonance condition. When the modal impedances are calculated, however, only one mode shows resonance, which is identified to be in relation with bus 9 once participation factor analysis is applied. Similar results are obtained when there are multiple capacitors in the system, i.e. the number of modes that show resonance are the same as the number of capacitors in the system, and each mode contains only one resonance.

For the original IEEE 14-bus network, the magnitude of the maximum modal impedance at each bus for each harmonic order is evaluated in [27] to construct the "critical mode" of the system, which can also be obtained as the largest eigenvalue of $\boldsymbol{Y}^{-1}$. For three specific modes, the critical mode is compared with the driving-point impedances of the most and least participating buses. In the comparison, it is found out that the impedances of the most participating buses have peaks coinciding with the peaks in the critical mode of the system, and the buses with the lowest participation factors associated with a specific mode do not show any peaks at the resonance frequencies of the modes.

In addition to their applications in power system resonance analysis, the two methods are commonly applied to resonance studies for traction networks. Their applications are compared in [59], in which the authors claim that the results obtained from the frequency scan study are redundant as all resonance peaks and valleys are seen equally important.

The two methods are further compared in [55, 56, 60, 61]. It is claimed in [56] that frequency scan analysis is inappropriate and ineffective for analyzing the parallel resonance frequencies of a system, as different nodal impedance curves yield non-identical resonant frequencies, which cannot easily be identified from the analysis results. In contrast, authors in [61] claim that frequency scan analysis is the best choice for a graphical resonance analysis that provides a "good understanding of the system's behavior at a glance", and HRMA is suitable for detailed analysis to locate the sources of resonances.

4.5 Conclusions

In this chapter, techniques to interpret the results obtained by applying the calculation methods introduced in Chapter 2 are discussed, and compared against each other. The following general recommendations can be made regarding the interpretation of results:

- A frequency scan study may, if modeling is done properly, closely match the actual harmonic impedances or voltage gains, as e.g., shown in [28, 7]. The existence of series and parallel resonances can be identified from the frequency scan results, by identifying valleys and peaks in the impedance, respectively. However, the frequency scan does not offer the possibility to detect the causes of the resonances.
- On the contrary, the results obtained from a HRMA study offer insights in the buses participating in the resonances whereas information related to gain magnitudes has no clear meaning. It has been used as a promising tool to complement the frequency scan results and provide further information on the causes of the resonances. The calculation of the eigenvectors and participation factors of the admittance matrix show the buses that are involved in a specific resonance, and, in a further step the effects of network parameters on the magnitude and frequency of the resonance can be traced.

In summary, the frequency scan study may be used to assess the magnitude of the driving-point or transfer-impedances, to identify series and parallel resonances and to assess their severity. The harmonic resonance mode analysis may be used to identify the buses participating in a certain resonance.

5

Frequency Domain Assessment of Severity of Cable Resonances

5.1 Amplification of Background Harmonics

Amplification of background harmonics due to grid resonances may lead to distorted voltage waves or excessive currents in equipment.

Amplification of background harmonics is typically assessed by comparing future voltage waveforms against reference voltage waveforms, as discussed in Section 2.5. Hereunder, we describe the methods for harmonic assessment as reported by several TSOs in the literature.

5.1.1 Current practice as reported in the literature

RTE RTE [10] focuses on amplification of voltage harmonics and uses field measurements in combination with simulations in EMTP-RV. They measure the line-to-neutral voltage harmonics in substations where cables are connected, for several weeks. The simulations in EMTP-RV consist of simulating a base-case with the actual grid configuration, and a "future" case in which the new project is modeled. According to [28], a 1A input current is injected and voltage waveforms for both cases are obtained for each frequency (no information is given on which type of waveforms are obtained, it is assumed that this has been done using frequency scan tool of EMTP-RV, which leads to a steady-state frequency solution). The voltage waveforms at the point-of-interest are compared for each frequency, and a gain is calculated as (see also Section 2.5):

$$G(\omega) = \frac{\text{Future voltage waveform}}{\text{Today's voltage waveform}}. \tag{5.1}$$

The measured harmonics are multiplied by this gain to assess the future harmonic profile. To take into account uncertainty on future parameters, a wide range of parameters and scenarios are considered (e.g., discussed in [28]. To limit the computational effort of consecutive time-domain simulations, the 400 kV grid, with parts of

the 225, 90 and 63 kV network, (totalling 4699 electrical nodes) is reduced into a frequency-dependent network equivalent. Results of the model validation phase show that the models accurately match the measurements. RTE mentions an uncertainty of +-10 Hz on the gain factors [28].

For the harmonic voltage distortion, RTE uses a limit of 4% of the nominal voltage. In the cases reported in [28], some scenarios led to the fifth harmonic reaching an amplitude of 9% of the nominal voltage.

EnergiNet Energinet [7] uses the voltage gain to assess the amplification of voltage harmonics in the 400 kV network to the 15 kV network. They have calculated the voltage gains using DigSilent PowerFactory with following models:

- Cables: Frequency-dependent phase models (available in PowerFactory) with manual implementation of cross-bonding;
- Transformers and shunt reactors: Only specified that they use frequency-dependent parameters;
- Wind farms: Thévenin equivalent which includes transformers and filters;
- Anholt island system: Distributed system with local loads on the island as CIGRE load model;
- 400 kV external grid: Thévenin representation where harmonic impedance is based on impedance polygons (300 points per polygon per harmonic are used). Polygons are constructed using a harmonic model of Danish transmission grid.

The calculated gains matched the ones which were obtained using measurements.

In [18], a method is described to analyze background harmonic amplification for various grid reinforcement projects. The steps are:

- Build a model (using the component modeling above).
- Determine scenarios to be investigated (e.g., different load scenarios, but also different filter configurations).
- Define harmonic current injection sources.
- Calculate bus voltages for each individual harmonic current injection source.
- Use the IEC summation law to add bus voltages calculated in previous step.
- Calculate voltage gain at all buses for each of the grid reinforcement projects, taking the voltage in the grid prior to the reinforcement as a base case. Compare the voltage gain to the IEC61000-3-6 planning level.
- Post-process the scenarios using a statistical analysis (e.g., divide into percentage quantiles and divide gains into problematic/non-problematic).

Energinet thus calculates voltage gains for each harmonic, and orders them into (i) significant amplifiction (gain>2), (ii) possible amplification (1.5<gain<2) and (iii) no amplification (gain<1.5). It thereby considers that the existing harmonics already use 50 % of the planning limit.

5.2 Temporary Overvoltages (TOV) due to resonance

5.2.1 Problems Associated with TOV

Temporary overvoltages may lead to accelerated aging or permanent equipment damage. They are defined as overvoltages of a few cycles of the fundamental frequency up to a few seconds. The effect of the overvoltages depends on the type of equipment [62]: (i) apparatus with a magnetic core (e.g., transformers or inductive VTs), (ii) linear devices without a core (e.g., circuit breakers, capacitor banks,...) and (iii) non-linear surge arresters. For the first type, the TOV withstand capability is mainly determined by thermal limitations. The TOV causes heating due to overexcitation of the core. For the second type, the TOV withstand capability is mainly determined by insulation parameters (except for capacitor banks). For the third type, the TOV withstand capability is determined by energy absorption capabilities. In [11], it is argued that the VTs are the most vulnerable equipment for short-duration TOVs (<0.7s) and surge arresters are the most vulnerable equipment for long duration TOVs (>0.7s).

The general method to assessing temporary overvoltages due to resonances is to first perform a frequency scan at the buses of interest to identify switching scenarios which may cause severe overvoltages (e.g., switching

scenarios which lead to parallel resonance peaks in the vicinity of 100 or 150 Hz). The switching scenarios are, e.g., taken as energization of a cable/line from both directions (closing one breaker) with a certain configuration (open/close) of the switches surrounding the line to be energized. Thereafter, a large number of time domain simulations (e.g., line or transformer energization) are performed on those switching scenarios which were identified by the frequency scan as problematic and the results are post-processed to assess whether any TOV limit is breached.

5.2.2 Series Resonance

In [3, 9], the procedure to analyze overvoltages due to series resonance is described as follows:

1. Find the most severe switching scenarios (by engineering judgment, e.g., by selecting those topologies which are anticipated to provide the most problems);
2. Find the dominant frequency contained in the cable energization overvoltage, by (Fourier analysis of a) time domain simulation or estimation using the cable characteristics;
3. Find the natural frequency of the series resonance circuit;
4. Study the difference between the two frequencies; dominant and natural frequency;
5. Simulate the most severe switching scenarios when the two frequencies are matched.

In step 2, the dominant frequency contained in the energization overvoltage can be obtained using time domain simulations or alternatively, via an estimation using the cable length ($f_n \approx v/(4 * l)$), or for long cables, a formulation found in the literature [4, 3]. In the latter formulation, the dominant frequency is calculated based on the assumption that (i) the cable is open-ended at one side) and (ii) the dominant frequency is associated with one of the intersheath modes rather than a coaxial mode. This assumption is justified by the fact that, in order for one of the coaxial modes to dominate, a critical frequency should be exceeded, and that this frequency for 400 kV XLPE cables is in the order of 1000-1500 Hz. The dominant frequency takes into account the cable system, as well as the source impedance connected to the closed end of the cable. A comparison of these formulations with a case modeled in PSCAD showed a good match.

In step 3, the series resonant frequency is obtained using a frequency scan at the bus connected to the switch to be operated. To study the propagation of the energization overvoltage to the lower voltage level, the input seen from the primary and transfer impedance seen from the primary of the transformer to the secondary of the transformer can be used to construct a voltage amplification factor (the voltage amplification factor can be found as the division of the transfer to the input impedance, i.e., similar to a voltage divider). If this factor is high, overvoltage at lower levels is highly likely during switching.

It should be noted that the series resonant frequency depends on system conditions, and therefore may be varied (within realistic ranges) to assess the most severe overvoltages.

In a study performed for Eirgrid [5], series resonances were found in general not to be problematic, even though TEPCO had experienced transformer failure during energization.

Example The circuit shown in Fig. 5.1 shows two cables, a grid represented by an inductor and a circuit Z_{eq} at a lower voltage level. The steps above are discussed consecutively:

1. In this example, a "most severe switching scenario" is chosen as energization of one cable with the other cable out of service.
2. In step 2, the dominant frequency contained in the cable energization overvoltage is estimated as $v/(4 * l)$.
3. In step 3, the natural frequency of the series resonance circuit is calculated through a frequency scan at bus 1. The series resonance is indicated by a valley in the input impedance.
4. In step 4 and 5, if the difference between the frequencies of step 2 and 3 is low, time domain simulations should be done. Prior to this, the voltage amplification factor from bus 1 to bus 2 may be found by dividing the transfer impedance from bus 1 to 2 by the input impedance at bus 1. If the voltage amplification factor is high, overvoltages due to series resonances are likely to occur.

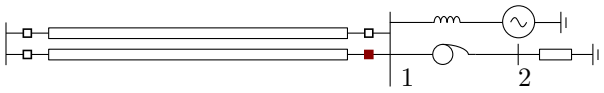

Figure 5.1: Example network for series resonance analysis.

5.2.3 Parallel Resonance

In [3, 5], parallel resonances due to transformer energization from a weak network are considered as leading to onerous overvoltages. A procedure for analyzing these overvoltages due to parallel resonance is described for a simplified circuit: in [3]:

1. Find the natural frequency of the parallel resonance circuit;
2. Set the natural frequency to 100 Hz by adjusting source impedances (or take those values of the external network harmonic impedance envelopes which lead to the lowest harmonic frequencies);
3. Simulate the most severe switching scenarios (transformer energization) with the natural frequency 100 Hz.

This procedure considers the source impedance to be an inductor, where the inductance value is determined based on the fault current level at the bus at which the cable is connected.

A more elaborate version of this procedure can be found in [5], where a larger part of the network around the bus of interest is modeled. The resonant frequencies of the parallel resonance circuit are calculated using a frequency scan.

In [11], a method for assessing the maximum permissible cable length is given. The procedure is as follows:

1. Network construction: The 400, 275 and 220 kV are modeled in detail (i.e., roughly in accordance to the modeling guidelines given in Chapter 3), whereas parts of the 110 kV system are also modeled in an EMT-type software.
2. Scenario selection: A large number of scenarios is considered, including seasonal variations.
3. Reactive power compensation: Shunt compensation is designed such that steady-state voltage limits are not breached.
4. Frequency scan: A frequency scan is performed to identify frequencies of potential resonant points.
5. TOV limit definition: Based on guidelines by IEC and IEEE, TOV limits are defined for equipment with magnetic cores, linear and non-linear equipment. VTs and surge arresters were found to be most vulnerable to TOV.
6. Time domain simulations for the critical cases to assess whether TOV limits are breached.

To increase the amount of cables in the system, mitigation methods such as a tuned filter were also considered. The frequency of the tuned filter was chosen based on the frequencies found in the frequency sweep.

To determine which cases to consider for time domain simulations, a harmonic impedance criterion is proposed in [10] and in [18]. The criterion in [10] is based on a simplified study of transformer energization against an RLC circuit. The simplified study takes into account probabilistic aspects concerning transformer energization. Based on the simplified study, a limit for the frequency domain impedance is constructed for each of the harmonic frequencies. This limit is based on a "global stress rate", which is an indicator taking into account the overvoltage stresses on the transformer and the surge arresters. In a second step, the harmonic impedance of the system connected to the transformer is determined. If the magnitude of this harmonic impedance is higher than the criterion based on the simplified transformer energization studies, then that topology is selected as a candidate for further detailed time-domain studies. A similar approach on thresholds is found in [18], several threshold values for 100, 150 and 200 Hz (+- 10 Hz) are specified based on knowledge of the Danish transmission system. These threshold values are 400, 600 and 2400 Ohms, respectively. An alternative criterion to determine which cases to consider for time domain simulation uses an index similar to the THD index [63]. It is important to note that the RTE approach as well as the approach discussed in [63] requires knowledge of the transformer energization phenomena, e.g., through a high-fidelity transformer model.

To reduce the dimensionality of the outputs of time-domain studies concerning temporary overvoltages, two new indicators to characterize temporary overvoltages are introduced in [64]. These indicators capture the RMS-value of the overvoltage as well as the peak value. They are designed to help in assessing TOV profiles obtained from EMT simulations, by reducing the time domain waveforms to these two indicators. The authors apply the method in [65] for a parametric study on harmonic filter design.

5.2.4 IEC 60007-1-4 on TOV

IEC 60007-1-4 [39] discusses in Sections 8.2 and 8.3 a fast (not recommended) and detailed calculation of temporary overvoltages. The detailed calculation of overvoltages uses the frequency domain to assess the events to be investigated and the time domain to simulate and analyze the events.

5.3 Summary

This section discusses the assessment of two potential problems associated with power system resonances, i.e., amplification of background harmonics and temporary overvoltages due to resonances.

5.3.1 Amplification of background harmonics

To assess harmonic background amplification, RTE and Energinet both calculate voltage gains. RTE multiplies the voltage gains with existing measured waveforms to obtain an estimate of the absolute voltage. This absolute voltage is compared against a limit of 4 % of the fundamental voltage waveform. Energinet classifies the voltage gains, and considers those above 2 as problematic. It thereby considers the IEC 61000-3-6 planning levels and assumes that 50 % of the planning level is already occupied as for today (meaning that gains above 2 result in harmonic voltages exceeding the planning level).

5.3.2 Temporary overvoltages due to resonances

Series resonances are identified as valleys in the driving-point impedances at the bus. A potential severe overvoltage at a lower level may exist if (i) at the primary system an overvoltage is generated at a bus due to series resonance and (ii) the frequency of this overvoltage matches the natural frequency of the lower level circuit. In the literature, in general, very few cases of such severe situations have been reported.

Parallel resonances are identified as peaks in the driving-point impedances at a bus. A potential severe overvoltage may occur if, e.g., a peak is located at a harmonic around 100-200 Hz, such that transformer energization may excite the parallel resonance. The assessment of parallel resonances may be performed by comparing the frequency domain response against a certain threshold. The limit on this threshold is reported in the literature as (i) based on operational experience, (ii) based on simulations of transformer energization against a simplified circuit. It should be noted that various values were found in different sources, but no clear agreement between those values was found.

It should be noted that, in general, the frequency domain assessment is used to indicate potential problem cases, whereas time-domain simulations are used for a complete analysis of these problem cases.

6

Mitigation Methods

This chapter provides a brief overview of mitigation methods as found in the literature [22, 52, 63, 66, 67]

6.1 Mitigation of Harmonics

Different methods exist for mitigating problems associated with harmonics [52]:

1. Design the system to withstand the effects of harmonics
2. Install filters or other mitigation devices close to the source of the harmonics
3. Reduce the generation of harmonics by, for example, increasing operation with higher pulse numbers, active wave-shaping techniques, etc.

6.1.1 System Reinforcement/Isolation Transformers

Harmonic distortion can be decreased by tuning the system impedance away from any parallel points [68], typically by increasing the strength of the system. Modifications to the system could include the commissioning of a power transformer. These will be more significant projects with long term effects on the grid and need to be analysed in depth.

In [69] the authors propose removing existing shunt capacitors in locations where new cables will be installed because the cable inherently already has a high capacitance. Alternatively, replacing shunt capacitors with C-type filters could add additional damping to higher frequencies.

Isolation transformers can also be installed, e.g., to deal with triplen harmonics (which are odd multiples of the third harmonic (3, 9, 15, 21)). Establishing a wye-delta connection can direct the triplen harmonics to the neutral connector.

6.1.2 Filters

Passive Filters

Passive filters may be a cost-effective solution to mitigate resonance problems, albeit that grid operation becomes more complex and their effectiveness may reduce when the grid impedance changes due to grid expansions [68]. The design of a passive filter consists of multiple capacitive and inductive components that are tuned to resonate at the desired frequency, or may even be a single reactor [68]. An example of a shunt filter is a C-type filter which has the advantage of having no losses at the fundamental frequency and better performance at higher frequencies. However, at extra high voltages, the physical dimensions of the filter components may form additional constraints [65].

Selecting the appropriate filter size will be a balance of cost and effectiveness. Commonly, a non-linear load will produce several harmonics. It is possible to install one large filter that will cover most of the requirements of the system. However, this would mean a much larger size of the filter, which could lead to significantly larger costs [52]. It is advised to install several smaller filters tuned to the problematic harmonics where the total installed compensation will be less than using one large filter [52, 70].

The system impedance determines the design of the passive filter. Therefore, if the system impedance changes, then the design of the filter may no longer be appropriate. For larger filters, the damping from the resistance could also increase the number of losses in the system. Finally, ageing might detune the resonance frequency over time.

Active Filters

Active filters are typically applied at the source of the harmonics. An active filter measures the harmonic distortion in a current waveform and generates a current equal current with 180 degree phase shift to revert the distorted voltage into a clean sinusoidal signal [52]. Active filters can cancel frequencies from the 2nd harmonic to the 50th and are capable of reducing the THD to less than 5% [71]. Active filters are connected in series, shunt, or a combination of both. Shunt active filters are targeted towards current harmonics, reactive power, and load current unbalance. They can be modeled as a current source. Series active power filters eliminate harmonic voltages and can be modeled as a voltage source.

Active filters overcome the shortcomings of the passive filters by not being susceptible to a change in the system impedance. Although the technology is mature also for high-voltage networks, they are often more costly and involve a higher complexity (due to the power-electronic components and controls) compared with passive filters. The most common active filter is a STATCOM or SVC compensator.

6.1.3 Limiting Harmonic Injections

By setting high standards on utilities and industries to limit the harmonic injection into the grid the risk for problems during resonance conditions might be mitigated. This is done by measuring the harmonics being produced at the source of non-linear loads or by designing components correctly so that they are operating at their rated power levels.

6.2 Mitigation of Temporary Overvoltages

Some common mitigation measures found in the existing literature to mitigate temporary overvoltages are [22, 63, 66, 67]:

- Limiting the cable lengths such that the impedance spectrum at the bus has no resonant frequencies below 150 Hz [6].
- Increase arrester voltage ratings, which causes more stringent constraints on insulation coordination. As surge arresters are not designed to withstand the relatively long TOV, this is not a recommended practice [6].
- Use shunt filters to suppress the low-frequency resonances [11, 65].
- Avoiding switching scenarios which may lead to TOV, e.g., by ensuring that alternative paths exists for transformer energization apart from a cable system [22].

- Point-on-wave switching or resistance switching: by controlling the angle at which the circuit breakers are switched in, or by adding a parallel resistance to the breaker, the overvoltages may be reduced [66].
- Neutral grounding reactor: although the neutral grounding reactor does not change the impedance spectrum, it might have a lowering effect on the overvoltages [72].
- Increasing the system loading: increasing the system loading adds damping to the system [22]. In [72], the resonance peak decreases from 16 kOhm to 8 kOhm when adding load to the system.
- Increasing the amount of classic generation: increasing the amount of generation shifts the resonances away from the low frequency region (especially during black start) [22, 63].
- Lowering the source voltage: lowering the source voltage may reduce the transformers' inrush current magnitudes [22, 63].

6.3 Practical Examples

A case study on the Northern Ireland EHV grid showed a parallel resonance peak close to the 2nd harmonic for 220 kV voltage level when 30 km of underground cables are added to the existing system. The initial time domain simulation of switching events showed that TOV was sufficient to cause harm. However, mitigation strategies could be implemented to reduce the severity. The proposed mitigation strategy was to implement a filter tuned to the resonance peak and placed close to the source of the resonance condition. This resulted in a 50 Mvar high pass filter with a tuned frequency of 143 Hz. After the implementation of the filter, the TOV was found to be within acceptable limits [68].

In [65], a parametric study on the design of C-type filters is performed. To design the C-type filters, they apply the method as described in 5.2.3. The authors conclude that design constraints for filters applied at 220 kV are lower compared to 380 kV. In the latter case, high filter ratings (in terms of MVAr) and high values for damping resistors are needed to sufficiently suppress TOVs. As an example, for the 380 kV, reactors with inductances around 500-800 mH were needed whereas in the 220 kV system, the required reactors had an inductance starting at approximately 175 mH..

In [69] the authors compare the effectiveness of using either a STATCOM or C-type filter to lower the parallel resonance peak at the third harmonic in a high voltage network in the United States. Frequency scans of the network showed that both devices shifted the impedance peak to the 4th harmonic but only the C-type filter lowered the impedance at the 3rd harmonic. An increase in the 3d harmonic impdance was noted for the STATCOM solution beyond the original peak (this increase was "on the way" to the fourth peak). It should be noted that for this study, the STATCOM was not equipped with active filtering. The study in [69] is based on the one done by KEMA in [17].

6.4 Summary

Mitigation methods to deal with background harmonic amplification and temporary overvoltages due to resonances introduced by cables may be categorized into (i) avoiding the phenomenon, (ii) suppressing the phenomenon or (iii) adapting the grid components to the phenomenon.

For background harmonic amplification, most mitigation techniques aim at suppressing the phenomenon, i.e., limiting harmonic injections, using filters or increasing system strength.

For temporary overvoltages, limiting the length of cables installed in the system, avoiding certain switching scenarios or using point-on-wave switching (for transformer energization) may be used to avoid the phenomenon. Suppressing the phenomenon can be done by (i) installing filters, (ii) increasing loading during switching, (iii) increasing traditional generation during switching, (iv) lowering source voltage during switching. To adapt grid components to the phenomenon, surge arrester ratings may be increased (although this is not recommended in literature).

It should be noted that certain mitigation methods may introduce increased complexity in operating the grid (e.g. applying filters), and may interfere with other grid phenomena (e.g. increased system strength leads to increased short-circuit currents or adapting surge arrester ratings may interfere with overvoltage management).

7

Example Case

In this chapter, a case study is performed to demonstrate the calculation methods and to illustrate the frequency shifts associated with the introduction of cables into the system. The case study is not a complete system study and results shown depend on the assumptions stated below.

⚠	The case study is not representative of a complete study of background harmonic amplification or temporary overvoltage assessment, but only represents the first step. Complete analysis methods are introduced in Chapter 5.
⚠	Although the test system shows great resemblance to the actual grid of Elia in West- and East-Flanders, the study performed here has limitations and study results should not be used for any purposes other than the demonstration of calculation methods and preliminary indications of shifts in the grid's frequency response.
⚠	The models used below are simplified. For a practical study, the guidelines according to chapter 3 should be used.
⚠	Although in a practical case study, the shunt reactors should be designed such that steady-state voltage limits are not breached, this is not done in the impedance analysis.

In the example case study, two cases are considered:

Case (i) In this case, the transmission lines between GEZEL380, IZGEM380 and AVLGM380 are overhead lines. This is the base case.

Case (ii) In this case, the transmission lines between GEZEL380 and IZGEM380 are cables, whereas those between IZGEM380 and AVLGM380 are overhead lines. Compared to the base case, a double circuit of cables (each circuit with length 52 km) is added.

The results of the base case (Fig. 7.1 and Fig. 7.2) show that

- The peaks in the sequence impedances do not necessarily coincide with the peaks in the diagonal elements of the phase impedances. This is due to the fact that the positive sequence impedance is a combination of the on- and off-diagonal elements (e.g., compare the phase impedances and positive sequence impedance around $f = 1000$ Hz in Fig. 7.1a).
- A frequency scan at a single bus may not reveal information on all possible resonances. For instance, the frequency peak in Z_{44} around $f = 2000Hz$ is not as pronounced in Z_{11}.
- Buses with high participation factors at a certain frequency also show peaks in their frequency scan (e.g., the positive sequence impedance of Z_{88} and participation factor PF_{8c} are simultaneusly high around $f = 1100Hz$ in Fig. 7.4)
- The modal analysis does not indicate series resonances.

In the example study, the (positive sequence) self impedance at bus 1 of the base case (Fig. 7.1a) shows several resonance peaks, e.g., around 140 Hz (peak 1), 655 Hz (peak 2) and a peak around 1005 Hz (peak 3). The positive sequence self-impedance at buses 2, 7 and 8 (Fig. 7.1b, c, d) show a peak around 1200 Hz (peak 4). For peak 1, all 380 kV buses except buses 8 and 9 have a similar value for the participation factor (Fig. 7.2c). For this peak, buses 8 and 9 have a lower participation factor. Peak 2 recurs also in $Z_{10,10}$ (not shown), and the modal analysis shows that the participation factor for bus 10 associated with the mode at 655 Hz is the highest. For peak 3, the participation factors of buses 7 and 8 are the highest, whereas for peak 4, bus 4 also participates (Fig. 7.2c). The series resonance seen in Z_{11} (Fig. 7.1a) is not reflected in the results of the modal analysis (Fig. 7.2b).

The comparison of frequency scans for Z_{11} of the different cases shows that:

- Increasing the amount of cables in the grid reduces the frequency at which the first resonance occurs (in this case from 150 Hz to 90-100 Hz)
- Increasing the amount of cables introduces a second peak in the frequency region below 1000 Hz (around 700-800 Hz).
- Increasing the amount of cables introduces more frequencies at which series resonance may occur.

When comparing the modal analysis for the different cases in the region 0-2500 Hz, following can be concluded:

- Increasing the amount of cables shifts the frequencies of the modes to the low frequency region.
- Adding cables to the same bus as a bus where cables are already attached (e.g, Case (ii)) may result in a preservation of a certain resonance frequency (e.g., the peak around 1000 Hz remains the same for case (i) and case (ii)), but changes the other peaks. To verify whether this is specific to this topology, this result should be verified on other topologies.
- The peak around 2000 Hz is more or less the same in both cases studied.

Finally, in Fig. 7.1a, three regions (100, 150 and 200 ± 10 Hz) are indicated, which may be used to track potential problem cases. For each of these regions, as outlined in Chapter 5, a limit on the amplitude of the impedance may be applied. Whenever the driving-point impedance exceeds this limit, a problematic case may be identified and further investigations (e.g., using time-domain simulations) may be performed for this case.

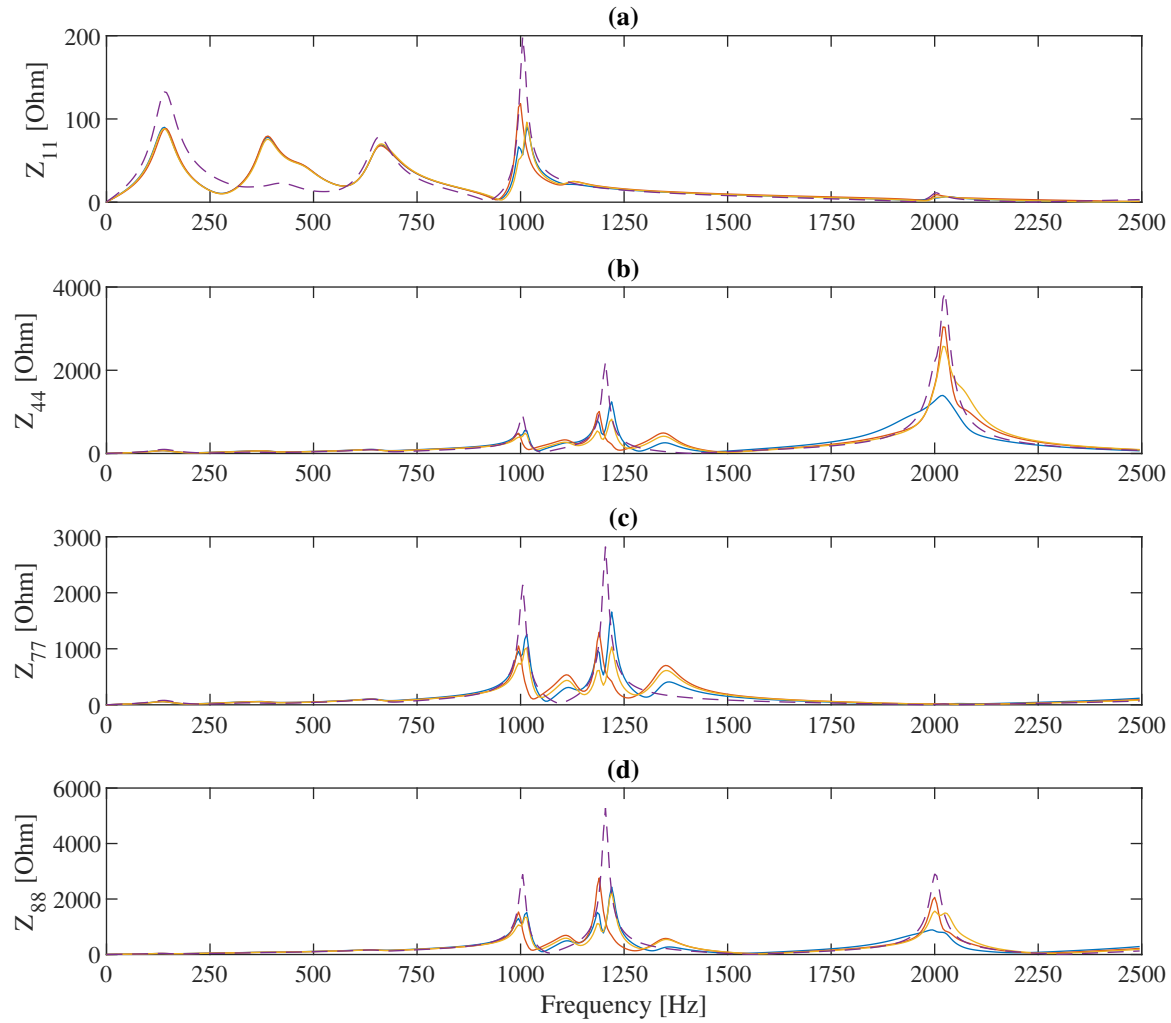

Figure 7.1: Selected elements from impedance matrix for base case (solid lines: phase impedances, dashed lines: positive sequence impedances). Indication of frequency regions within which limits on the amplitude may be applied in preliminary screening studies for temporary overvoltages.

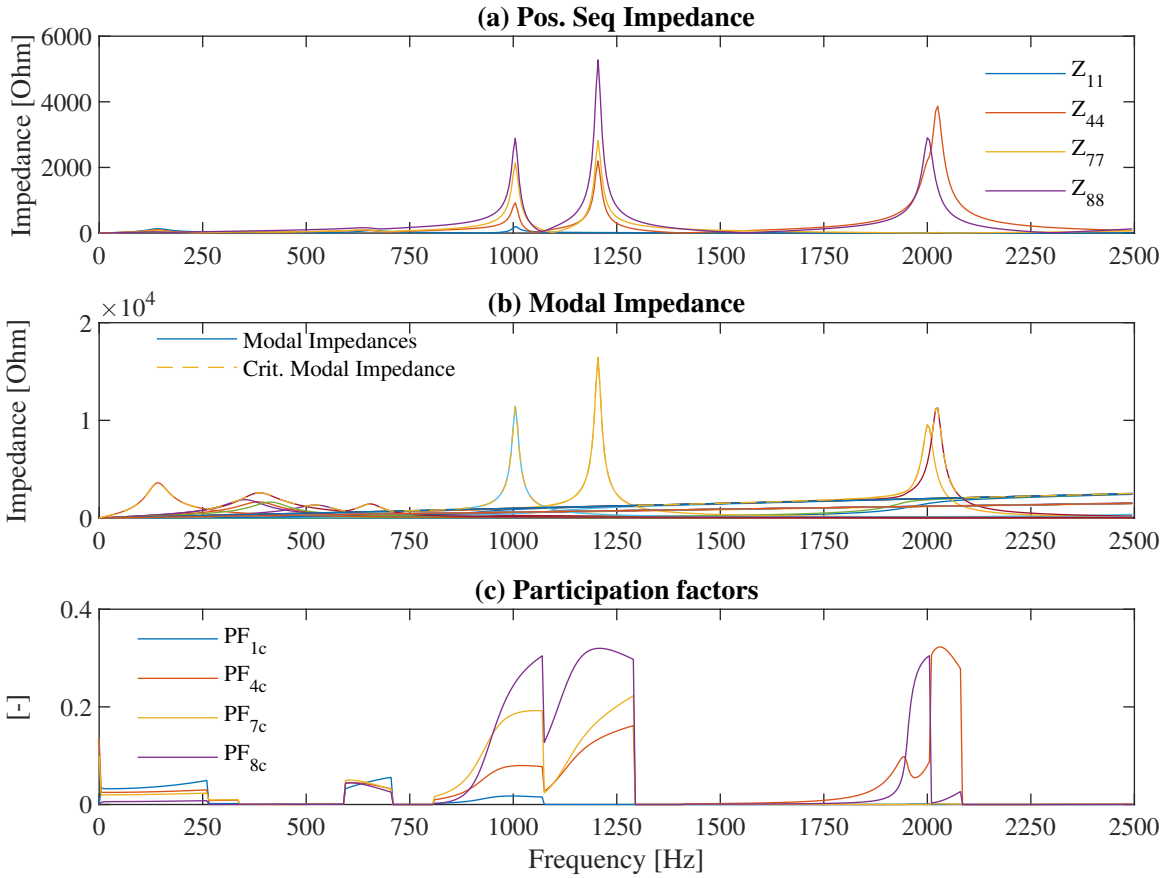

Figure 7.2: Magnitudes of the modal impedances for base case.

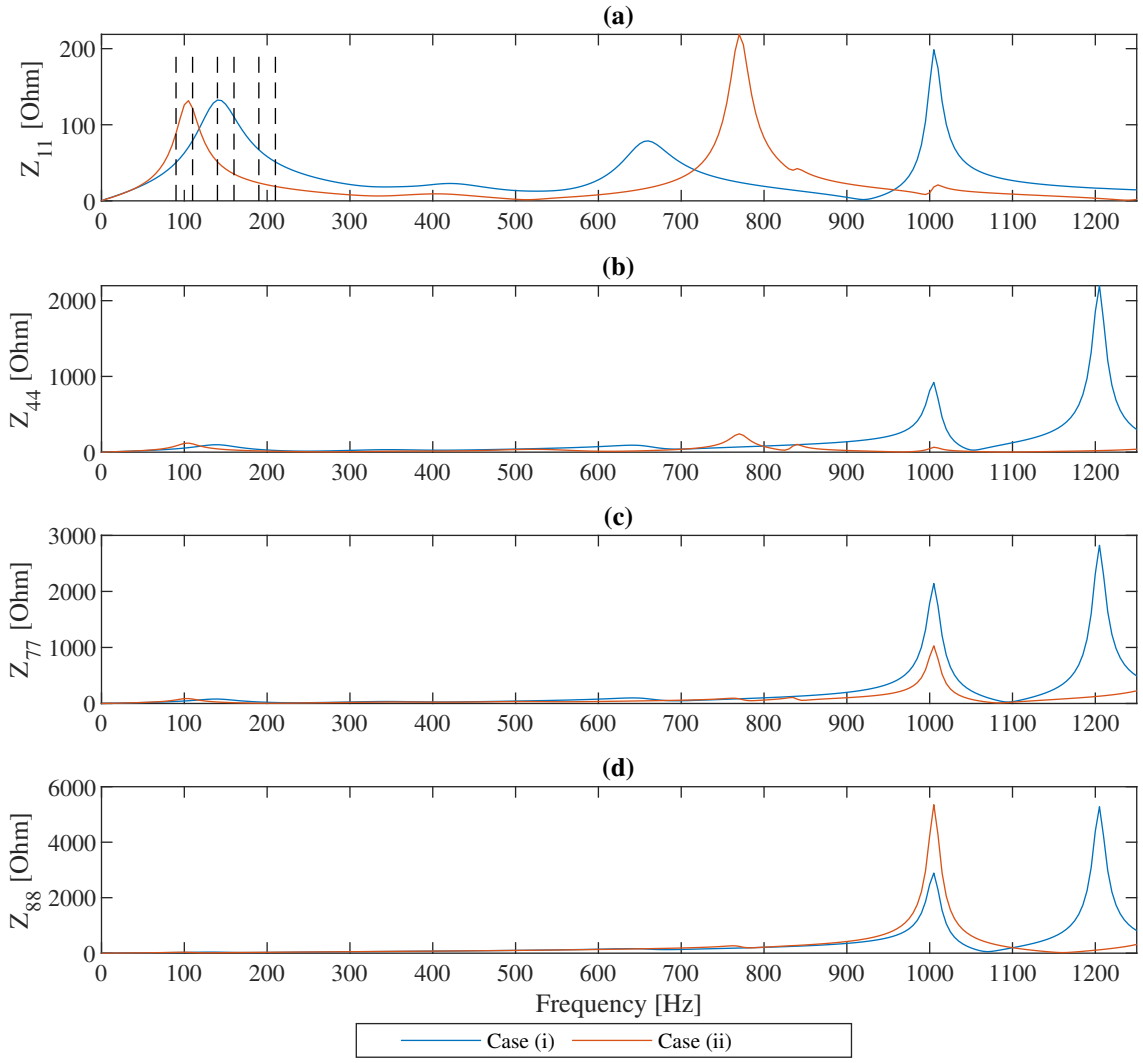

Figure 7.3: Selected elements from impedance matrix for both cases (positive sequence only).

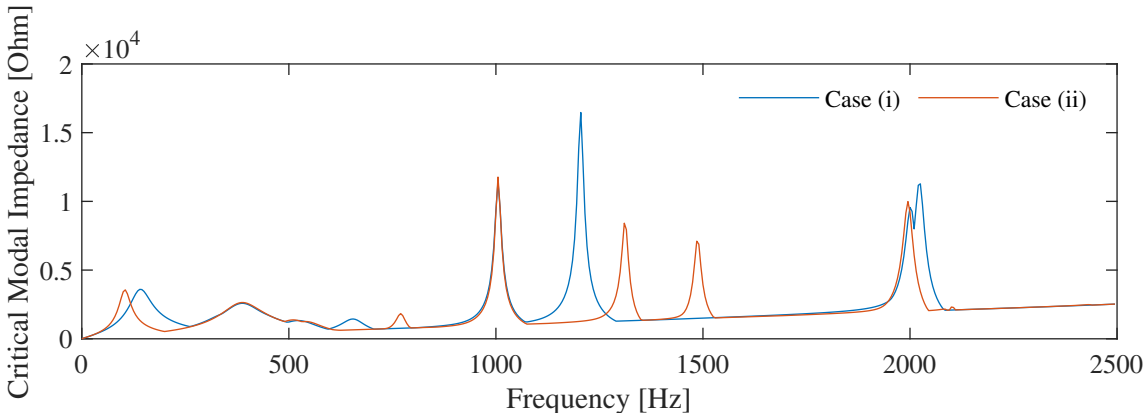

Figure 7.4: Magnitudes of the modal impedances for both cases.

8

Conclusion

Cables have been acknowledged by transmission system operators as one of the factors contributing to amplification of background harmonics or temporary overvoltages during switching events The origins of these problems lies in the shift of existing resonances to lower frequencies, caused by the increase in capacitance due to adding cables to the grid. Therefore, existing background harmonics present at those lower frequencies may be amplified to unacceptable levels, leading to e.g. power quality problems at lower voltage levels. For temporary overvoltages, the lower resonant frequencies may coincide with harmonics injected during switching events (e.g., the low-order harmonics during transformer energization). These temporary overvoltages were found to prevail especially during switching events in weak systems or in systems with a large amount of cables. An example case study in this document confirmed that increasing the amount of cables caused a shift of existing resonances to lower frequencies as well as an increase of resonance peaks in the frequency region up to 2500 Hz.

Industry practice shows that background harmonic amplification is assessed by means of harmonic voltage gains, expressing the gain of the existing background (voltage) harmonics to the ones anticipated in future grid situations. The voltage gains may be (i) compared against planning levels (assuming the existing harmonics already use part of that planning level) or (ii) may be multiplied with measured harmonic voltage waveforms to assess the absolute harmonic level in future grid situations. Uncertainty on the frequency of the voltage gain (e.g. ± 50 Hz) should be taken into account in the assessment.

Frequency scans of the driving-point impedance may indicate problematic cases of temporary overvoltages caused by series and parallel resonance phenomena, e.g., in a screening study, but should be complemented by time domain studies in a further assessment. A focus may be put on parallel resonance, as the consulted literature indicated a relatively low amount of problematic series resonance cases. A frequency domain assessment of parallel resonances consists of comparing the driving-point impedance against a certain threshold at selected frequencies (e.g., 100-150-200 Hz). The threshold is constructed using (i) TOV limits for equipment such as surge arresters or transformers and (ii) transformer energization characteristics. Thresholds on the impedance were selected at the minimum impedance (for each selected frequency) beyond which surge arresters or transformers would sustain damage. It should be noted that different sources mention various values for the thresholds, but no clear agreement between those values was found. A complete assessment of problematic cases as indicated by the frequency domain assessment typically involves complementary studies in the time domain, which are typically more time consuming. The frequency domain assessment can therefore be used to limit the amount of

cases to be studied in the time domain.

The overview of mitigation techniques to deal with background harmonic amplification and temporary overvoltages due to resonances presented in Chapter 6 resulted in the following options for harmonic compensation and temporary overvoltage management. For harmonic compensation, the options found in literature are (i) system design to increase the system inductance, (ii) passive filters, (iii) active filters and (iv) limiting harmonic injections. For temporary overvoltage management, following options were found: (i) avoiding switching scenarios which lead to problems (e.g., increasing load, increasing generation, avoiding transformer energization through a cable), (ii) using shunt filters, (iii) point-on-wave switching, (iv) neutral grounding reactors, (v) lowering the source voltage during switching. These mitigation methods may be categorized into (i) avoiding the phenomenon, (ii) suppressing the phenomenon or (iii) adapting the grid components to the phenomenon. It should be noted that some mitigation methods may introduce increased complexity in planning and operating the grid (e.g. applying filters), or may interfere with other grid constraints (e.g. increased system strength leads to increased short-circuit currents).

Besides the analysis of severity assessment and mitigation methods used within the industry, this report serves as a reference work for calculation methods (Chapter 2), modeling for resonance analysis (Chapter 3) and result interpretation (Chapter 4). Chapter 2 outlines the calculation methods which are commonly used for resonance analysis, i.e., frequency scan and harmonic resonance mode analysis, from which methods may be derived such as voltage scan or voltage gain calculations. Chapter 3 provides guidelines for modeling of components, with in accordance to the project scope, an emphasis on passive components rather than active components, and for modeling the network. The main conclusion from Chapter 3 is that resonance studies require an extensive amount of the system to be modeled in detail, and that models should ideally reflect frequency-dependency of parameters. This requires knowledge of component parameters beyond the studies done for 50 Hz. In Chapter 4, the frequency scan and harmonic resonance mode analysis are compared. The frequency scan method provides accurate estimates of the magnitude of the driving-point or transfer-impedances whereas the harmonic resonance mode analysis may be used to localize the sources of resonance.

An overview of the problems, assessment- and mitigation methods as discussed in this report are found in Table 8.1.

As a final note, the literature review reveals that practical resonance studies generally take into account the uncertainty associated with input parameters and modeling choices through e.g. model validation (for instance, in combination with measurement campaigns) and appropriate scenario selection.

Phenomenon	Example Causes	Frequency Range	Freq. Domain Indicators	Assessment	Mitigation
Background harmonic amplification	Voltage gain shift/increase due to cable insertion	E.g. 5th-7th-11th-13th harmonic [18]	Voltage gains at harmonic frequencies	Combined frequency domain modeling and measurements	System design, filtering or limiting of harmonic injections
Series Resonance Overvoltages	Energization of cable	Depends on cable length	Match between network series resonant frequency and resonant frequency at lower level network	Screening in frequency domain (series resonances and voltage gains) and further assessment in time domain studies	[In consulted literature (mainly) not considered problematic]
Parallel Resonance Overvoltages	Transformer energization in weak cable system	100-150-200 Hz [18] or 50-1000 Hz [10]	Driving-point impedance magnitude exceeding limits at specified frequencies	Screening in frequency domain, assessment in time domain studies	Switching sequences, point-on-wave switching, filtering, increased loading before energization

Table 8.1: Overview of problems associated with resonance phenomena and findings from the literature.

Bibliography

[1] M. H. J. Bollen and S. M. Gargari, "Harmonic resonances due to transmission cables," in *Proc. CIGRE Belgium*, Brussels, Belgium, Mar. 2014.

[2] CIGRE WG C4.307, "Resonance and Ferroresonance in Power Networks," CIGRE, Technical Brochure TB 569, 2013.

[3] A. Ametani, T. Ohno, and N. Nagaoka, *Cable System Transients*. Singapore: J. Wiley & Sons, 2015.

[4] T. Ohno, C. L. Bak, A. Akihiro, W. Wiechowski, and T. K. Sorensen, "Derivation of Theoretical Formulas of the Frequency Component Contained in the Overvoltage Related to Long EHV Cables," *IEEE Transactions on Power Delivery*, vol. 27, no. 2, pp. 866–876, Apr. 2012.

[5] Tokyo Electric Power Company, "Assessment of the Technical Issues relating to Significant Amounts of EHV Underground Cable in the All-island Electricity Transmission System," Tokyo Electric Power Company, Public Report, Nov. 2009.

[6] CIGRE WG C4.502, "Power system technical performance issues related to the application of long HVAC cables," CIGRE, Technical Brochure 556, Oct. 2013.

[7] C. Jensen, "Harmonic Background Amplification in Long Asymmetrical High Voltage Cable Systems," in *Proc. IPST 2017*, Seoul, Korea, Jun. 2017.

[8] W. Wiechowski and P. Borre Eriksen, "Selected studies on offshore wind farm cable connections - challenges and experience of the Danish TSO," in *Proc. 2008 IEEE PES GM*, Pittsburgh, PA, USA, Jul. 2008, iSSN: 1932-5517.

[9] T. Ohno, "Dynamic Study on the 400 kV 60 km Kyndbyværket – Asnæsværket Line," PhD Thesis, Aalborg University, Aalborg, Denmark, Dec. 2012.

[10] Y. Vernay, S. Deschanvres, and Y. Fillion, "RTE experiences with the insertion of long EHVAC insulated cables," in *Proc. CIGRE 2014*, Paris, France, Aug. 2014.

[11] N. Cunniffe, M. Val Escudero, A. Mansoldo, E. Fagan, M. Norton, and C. Ellis, "Investigating the Methodology and Implications of Implementing Long HVAC Cables in the Ireland and Northern Ireland Power System," in *Proc. CIGRE 2016*, Paris, France, Aug. 2016.

[12] L. Wu, "Impact of EHV/HV underground power cables on resonant grid behavior," Ph.D. dissertation, TU Eindhoven, Eindhoven, The Netherlands, Oct. 2014.

[13] G. Hoogendorp, "Steady State and transient behavior of underground cables in 380 kV transmission grids," PhD Thesis, TU Delft, Delft, The Netherlands, Oct. 2016.

[14] H. Khalilnezhad, "Technical Performance of EHV Power Transmission Systems with Long Underground Cables," Ph.D. dissertation, TU Delft, Delft, The Netherlands, 2018.

[15] F. Barakou, "Investigation of the impact of EHV underground power cables on the resonant and transient grid behavior," Ph.D. dissertation, TU Eindhoven, Eindhoven, The Netherlands, 2018.

[16] K. Jansen, B. van Hulst, C. Engelbrecht, P. Hesen, K. Velitsikakis, and C. Lakenbrink, "Resonances due to long HVAC offshore cable connections: studies to verify the immunity of dutch transmission network," in *2015 IEEE PowerTech*, Eindhoven, The Netherlands, Jun. 2015, pp. 1–6.

[17] J. Enslin, R. Wakefield, Y. Hu, and S. Eric, "Harmonic Impedance Study for Southwest Connecticut Phase II Alternatives," Tech. Rep., Oct. 2004.

[18] Energinet, "Technical Issues Related To New Transmission Lines in Denmark," Tech. Rep. Doc. 18/04246-24, Sep. 2018.

[19] IEEE Std 519™-2014, "IEEE Recommended Practice and Requirements for Harmonic Control in Electric Power Systems," IEEE, Tech. Rep. IEEE Std 519™-2014, 2014.

[20] IEEE Std 519 - 1992, "IEEE Recommended Practices and Requirements for Harmonic Control in Electrical Power Systems," IEEE, Tech. Rep., 1992.

[21] CIGRE WG B4.47, "Special Aspects of AC Filter Design for HVDC Systems," CIGRE, TB 568 Addendum to Technical Brochure 139, Oct. 2013.

[22] CIGRE WG C4.307, "Transformer Energization in Power Systems: A Study Guide," CIGRE, Tech. Rep. 568, 2014.

[23] CIGRE JWG C4/B4.38, "Network modelling for harmonic studies," CIGRE, Tech. Rep. TB 766, Apr. 2019.

[24] Zhenyu Huang, Wilsun Xu, and V. R. Dinavahi, "A practical harmonic resonance guideline for shunt capacitor applications," *IEEE Transactions on Power Delivery*, vol. 18, no. 4, pp. 1382–1387, Oct. 2003.

[25] T. Reveyrand, "Multiport conversions between S, Z, Y, h, ABCD, and T parameters," in *Proc. INMMIC*, Brive La Gaillarde, France, Aug. 2018.

[26] D. Frickey, "Conversions between S, Z, Y, H, ABCD, and T parameters which are valid for complex source and load impedances," *IEEE Transactions on Microwave Theory and Techniques*, vol. 42, no. 2, pp. 205 – 211, 1994.

[27] Wilsun Xu, Zhenyu Huang, Yu Cui, and Haizhen Wang, "Harmonic resonance mode analysis," *IEEE Transactions on Power Delivery*, vol. 20, no. 2, pp. 1182–1190, Apr. 2005.

[28] Y. Fillion and S. Deschanvres, "Background harmonic amplification within offshore wind farm connection projects," in *Proc. IPST 2015*, Cavtat, Croatia, Jun. 2015, 8 pages.

[29] PSCAD, *EMTDC User's Guide*. Manitoba HVDC Research Centre, 2010. [Online]. Available: https://hvdc.ca/uploads/ck/files/reference_material/EMTDC_User_Guide_v4_3_1.pdf

[30] DigSILENT, *DIgSILENT PowerFactory 2019 User Manual*. DIgSILENT GmbH, 2019. [Online]. Available: http://79.101.33.142/DIgSILENT%20PowerFactory%202019%20User%20Manual/UserManual_2019_en.pdf

[31] SIEMENS AG, "PSS SINCAL 13.0 Harmonics," 2016.

[32] A. Bayo Salas, "Control Interactions in Power Systems with Multiple VSC HVDC Converters," PhD Thesis, University of Leuven, Leuven, Belgium, Aug. 2018.

[33] J. Martinez-Velasco, *Power System Transients: Parameter Determination*. Boca Raton, FL: CRC Press, 2009.

[34] J. Marti, L. Marti, and H. Dommel, "Transmission line models for steady-state and transients analysis," in *Proc. IEEE APT '93*, Athens, Greece, Sep. 1993, pp. 744–750.

[35] S. Grivet-Talocia and B. Gustavsen, *Passive Macromodeling - Theory and Applications*. Hoboken, NJ: J. Wiley & Sons, 2016.

[36] J. R. Marti, "Accurate Modelling of Frequency-Dependent Transmission Lines in Electromagnetic Transient Simulations," *IEEE*, vol. PAS-101, no. 1, pp. 147–157, Jan. 1982.

[37] A. Morched, B. Gustavsen, and M. Tartibi, "A universal model for accurate calculation of electromagnetic transients on overhead lines and underground cables," *IEEE Transactions on Power Delivery*, vol. 14, no. 3, pp. 1032–1038, Jul. 1999.

[38] CIGRE WG 33.02, "Guidelines for Representation of Network Elements when Calculating Transients," CIGRE, Brochure TB 39, 1990.

[39] IEC TR and IEC 60071-4:2004, "Insulation co-ordination — Part 4: Computational guide to insulation co-ordination and modelling of electrical networks," IEC, Standard, 2004.

[40] Alvarez-Cordero, Gabriel, Bachiller Soler, A., Gómez-Expósito, A., Rosendo Macías, J. A., and Gómez-Simón, Cristina, "A methodology for harmonic impedance in large power systems. Application to the filters of a VSC," in *Proc. CIGRE 2012*, Paris, France, Aug. 2012.

[41] Working Group B1.30, "Cable Systems Electrical Characteristics," CIGRE, TB 531, 2013.

[42] A. Robert and T. Deflandre, "Guide for Assessing The Network Harmonic Impedance," *CIGRE Electra*, vol. 167, Aug. 1996.

[43] CIGRE WG 36-05, "Harmonics, characteristic parameters, methods of study, estimates of existing values in the network," *CIGRE Electra*, vol. 77, pp. 35–54, 1981.

[44] IEEE Std. 399-1997, "IEEE Recommended Practice for Industrial and Commercial Power Systems Analysis (Brown Book)," IEEE, Tech. Rep., 1997. [Online]. Available: https://standards.ieee.org/standard/399-1997.html

[45] J. Arrillaga, L. Juhlin, M. Lahtinen, P. Ribeiro, and A. Saavedra, "Ac System Modelling For Ac Filter Design - An Overview of Impedance Modelling," *CIGRE Electra*, no. 164, Feb. 1996.

[46] P. M. Anderson, *Analysis Of Faulted Power Systems*, ser. IEEE Press Power Systems Engineering Series. NY: John Wiley & Sons, 1995.

[47] J. Wasilewski, W. Wiechowski, and C. Bak, "Harmonic domain modeling of a distribution system using the DIgSILENT PowerFactory software," in *2005 International Conference on Future Power Systems*, Nov. 2005, pp. 7 pp.–7.

[48] IEEE Std. 3002.8-2018, "IEEE Recommended Practice for Conducting Harmonic Studies and Analysis of Industrial and Commercial Power Systems," *IEEE Std 3002.8-2018*, pp. 1–79, Oct. 2018.

[49] Task Force on Harmonics and Simulation, "Modeling and simulation of the propagation of harmonics in electric power networks. I. Concepts, models, and simulation techniques," *IEEE Transactions on Power Delivery*, vol. 11, no. 1, pp. 452–465, Jan. 1996.

[50] Luigi Colla, S. Lauria, and F. M. Gatta, "Temporary Overvoltages due to Harmonic Resonance in Long EHV Cables," in *Proc. IPST 2007*, Lyon, France, Jun. 2017.

[51] F. Barakou, M. H. J. Bollen, S. Mousavi-Gargari, P. A. A. F. Wouters, and E. F. Steennis, "Downstream network modeling for switching transients in EHV networks containing cables," in *Proc. IEEE PowerTech*, Manchester, UK, Jun. 2017.

[52] J. C. Das, *Power System Analysis: Short-Circuit Load Flow and Harmonics*, 1st ed. New York: CRC Press, Apr. 2002.

[53] S. Dennetière, A. Parisot, E. Milin, and A. D. Pons, "Resonance and insertion studies with EMTP: Working with large scale network models," in *Proc. International Conference on Power Systems Transients (IPST2011)*, Delft, The Netherlands, Jun. 2011.

[54] Y. Vernay and B. Gustavsen, "Application of Frequency-Dependent Network Equivalents for EMTP Simulation of Transformer Inrush Current in Large Networks," in *Proc. IPST 2013*, Vancouver, Canada, Jun. 2013.

[55] O. Galland, D. Leu, V. Berner, and P. Favre-Perrod, "Resonance Analysis of a Transmission Power System and Possible Consequences of its Undergrounding," *Periodica Polytechnica Electrical Engineering and Computer Science*, vol. 59, no. 3, pp. 88–93, Sep. 2015.

[56] C. Amornvipas and L. Hofmann, "Resonance analyses in transmission systems: Experience in Germany," in *Proc. IEEE PES GM*, Minneapolis, Minnesota, USA, Jul. 2010, pp. 1–8, iSSN: 1932-5517, 1944-9925, 1944-9925.

[57] A. Neufeld, N. Schäkel, and L. Hofmann, "Harmonic Resonance Analysis for Various Degrees of Cable Penetration in Transmission Grids," in *Proc. UPEC*, Glasgow, UK, Sep. 2018.

[58] M. Quester, M. Knittel, P. Raffelsiefen, and A. Schnettler, "Resonance Mode Analysis of Cabling in the Transmission System," in *Proc. UPEC*, Glasgow, UK, Sep. 2018, pp. 1–6.

[59] H. Hu, H. Tao, X. Wang, F. Blaabjerg, Z. He, and S. Gao, "Train–Network Interactions and Stability Evaluation in High-Speed Railways—Part II: Influential Factors and Verifications," *IEEE Transactions on Power Electronics*, vol. 33, no. 6, pp. 4643–4659, Jun. 2018.

[60] O. Galland, L. Eggenschwiler, R. Horta, W. Sattinger, P. Favre-Perrod, and D. Roggo, "Application of Resonance Analysis to AC–DC Networks," *IEEE Transactions on Power Delivery*, vol. 33, no. 3, pp. 1438–1447, Jun. 2018.

[61] A. Arasteh, O. Goksu, J. N. Sakamuri, and N. A. Cutululis, "On the Methods of Resonance Identification in Power Systems," in *Proc. IEEE 2019 PowerTech*, Milan, Italy, Jun. 2019, pp. 1–6.

[62] CIGRE WG 33.10, "Temporary overvoltage withstand characteristics of extra high voltage equipment." *CIGRE Electra*, no. 179, Aug. 1998.

[63] A. Ketabi, A. Ranjbar, and R. Feuillet, "Analysis and control of temporary overvoltages for automated restoration planning," *IEEE Transactions on Power Delivery*, vol. 17, no. 4, pp. 1121–1127, Oct. 2002.

[64] K. Velitsikakis and C. Engelbrecht, "Proposed Method for Evaluating Temporary Overvoltages in Transmission Systems due to Low Harmonic Order Resonances," in *Proc. CIGRE Dublin*, Dublin, Ireland, Jun. 2017, 10 pages.

[65] ——, "Application of C-type Harmonic Filters as Remedial Measure Against Temporary Overvoltages in Transmission Systems due to Harmonic Resonances," in *Proc. CIGRE 2018*, Paris, France, Aug. 2020, 10 pages.

[66] J. Das, *Transients in Electrical Systems*. McGraw-Hill, 2010.

[67] London Power Associates, "Investigation into Mitigation Techniques for 400/220 kV Cable Issues," Jan. 2015. [Online]. Available: http://www.eirgridgroup.com/site-files/library/EirGrid/Investigation-into-Mitigation-Techniques-for-Cable-Issues.pdf

[68] EirGrid, "An Information Note on Harmonic Issues and their impact on Customer connections," 2013. [Online]. Available: http://www.eirgridgroup.com/site-files/library/EirGrid/AnInformationNoteOnHarmonicIssuesv1.0.pdf

[69] R. Wakefield, Y. Hu, J. Enslin, R. Wakefield, Y. Hu, and J. Enslin, "System Considerations and Impacts of AC Cable Networks on Weak High Voltage Transmission Networks," in *Proc. IEEE T&D*, Dallas, TX, USA, May 2006, pp. 1030–1034, iSSN: 2160-8563.

[70] K. M. El-Naggar, H. M. Ismail, and M. Al-Fahd, "Harmonic modeling, analysis, mitigation of Kuwait EHV electrical network," *Electrical Engineering*, vol. 91, no. 3, p. 145, Sep. 2009.

[71] Z. Salam, T. P. Cheng, and A. Jusoh, "Harmonics Mitigation Using Active Power Filter: A Technological Review," *Elektrika*, vol. 8, no. 2, pp. 17–26, 2006.

[72] S. G. Kim, "Overvoltage Studies on ELIA's Stevin 380kV Cable Link (Part 1: TOV Switching Overvoltage Study)," Tech. Rep. R13-946, Oct. 2013.

A

Case Parameters

A.1 Example Test System

The example test system shown in Fig. A.1 is used only for demonstration purposes of the calculation methods and for indications regarding shifts in frequency response.

⚠	Although the test system shows great resemblance to the actual grid of Elia in West- and East-Flanders, the study performed here has limitations and study results should not be used for any purposes other than the demonstration of calculation methods and preliminary indications of shifts in the grid's frequency response.
⚠	The models discussed below are simplified. For a practical study, the guidelines according to chapter 3 should be used.

The assumptions within the study are:

- At the 380 kV buses MERCA380 and FR_EQ380, a fundamental frequency Thévenin impedance is added. The Thévenin impedance is purely inductive and resembles an external grid of 10 GVA.
- Loads are modeled directly at the secondary of the transformers. In a practical study, a frequency-dependent network equivalent should be used, or a part of the secondary network should ideally be modeled.
- The shunt compensation is left unaltered for the frequency scans, and is varied for the TOV studies.

A.2 Grid Equivalents

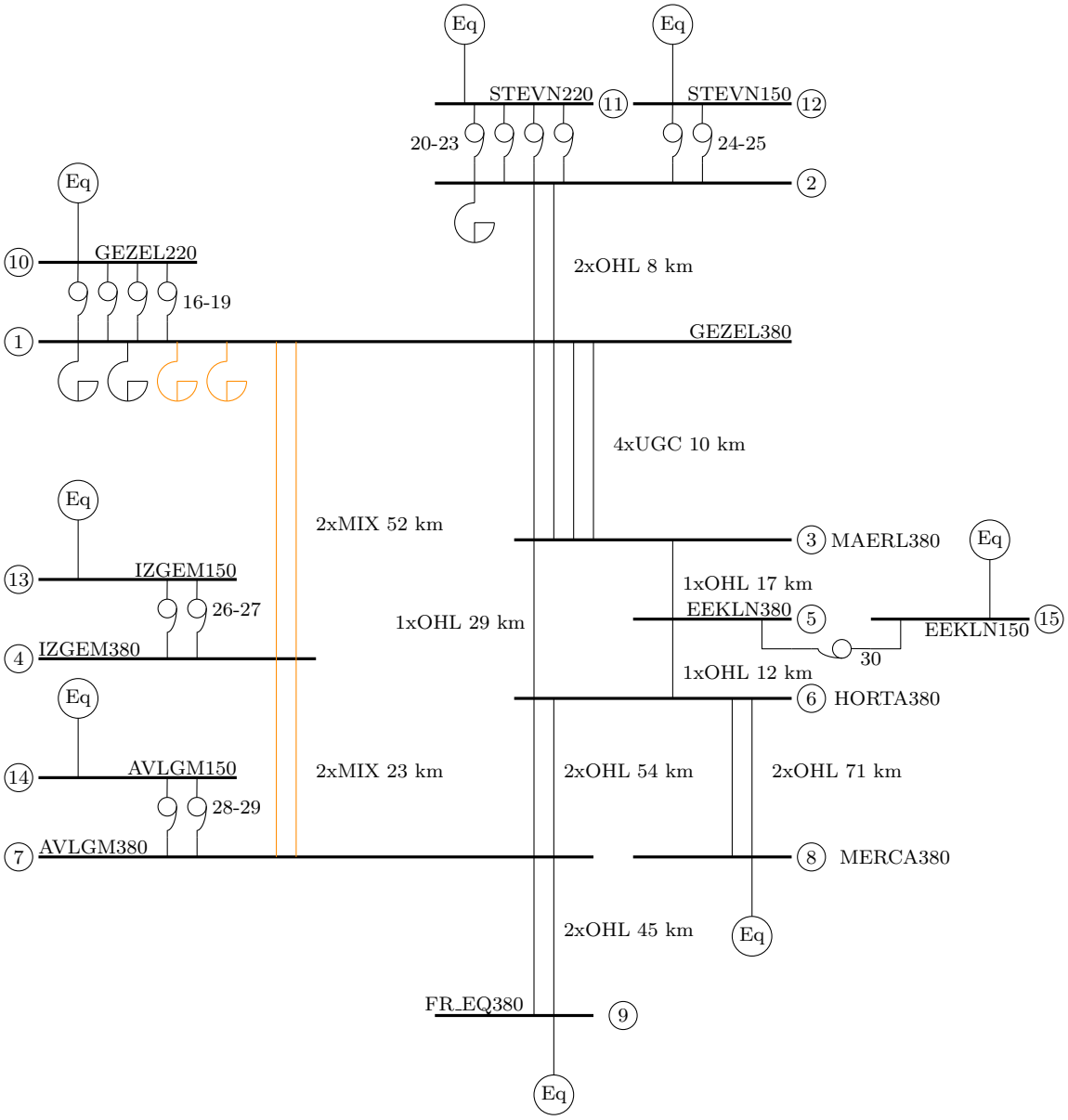

Figure A.1: Test system used in the examples

Table A.1: Cable parameters

Conductor	Inner Radius [mm]	Outer Radius [mm]	ρ [Ωm]	μ_r	ϵ_r
Core	0	31.75	2.18e-8	1	-
Inner Semiconductor	31.75	33.75	-	-	-
Main Insulation	33.75	59.55	-	-	2.26
Outer Semiconductor	59.55	60.85	-	-	-
Metallic Screen	60.85	61.05	1.72e-8	1	-
Outer Sheath	61.05	65.95	-	-	2.26

The grid equivalents, representing a system with a short-circuit level of approximately 10 GVA, are modeled as an inductor of value 0.05 H. In a practical study, a frequency-dependent grid equivalent should be used and the impedance of the grid equivalent should vary with the operating conditions. Alternatively, a larger part of the primary system should be modeled such that the fundamental frequency grid equivalent is far enough from the area of interest (study zone).

A.3 Cables

The cables are modeled as an arrangement of multiple single core cables (depending on the number of parallel circuits). The cable geometry and material parameters for a single core are given in Table A.1. The earth resistivity is set to 25 Ωm. The burial depth of the cables is 1.9 m. Each cable within a three-phase circuit has an inter-core distance of 0.5 m and the distance between the cores of the same phase within each circuit is 2.32 m. The cables sheaths are cross-bonded and at the sheaths are at the end of each cross-binding triplet short-circuited and earthed. The total length of 1 minor section is lower than 900 m.

The cables are modeled using a frequency-dependent phase model. The cross-bonding is modeled either explicitly (exact solution) or as ideal cross-bonding (approximate solution).

The length of a minor section of the cables between GEZEL380 and MAERL380, is 834 m and four major sections are used, leading to a length of 10 km. The length of a minor section of the cables between and IZGM380 is 866.7 m and 20 major sections are used. The length of a minor section of the cables between IZGM380 and GEZEL380 is 851.9 m and 9 major sections are used, leading to a length of 23 km.

A.4 Overhead lines

The overhead lines are single- or double circuit overhead lines with conductor parameters and line geometry as given in Table A.2. For a single-circuit overhead line, only one circuit (e.g., 1-3) is used. The ground resistivity is 25 Ωm.

A.5 Transformers

The transformers are autotransformers with a YNa0(d) winding configuration. The transformer parameters are given in Tables A.3 and A.4.

The transformers are modeled by a simplified circuit according to the guidelines given in Section 3.2. Copper losses are neglected.

A.6 Loads

At the 220 and 150 kV buses, loads are modeled as a parallel RX-circuit, either capacitive or inductive. At the 220 kV buses, the load is assumed to have an active and reactive power of 250 MW and 125 MVAr, respectively.

Table A.2: Overhead Line Parameters

Conductor	X [m]	Y [m]	Sag [m]	Conductor Radius [m]	Number of Bundles	DC Resistance [Ohm/km]
1	-7	30	10	.016	4	.05
2	-7	39	10	.016	4	.05
3	-7	48	10	.016	4	.05
4	7	30	10	.016	4	.05
5	7	39	10	.016	4	.05
6	7	48	10	.016	4	.05
GW1	-4	57	10	0.011	4	.1
GW2	4	57	10	0.011	4	.1

Table A.3: Transformer A parameters

Nominal Power	555 MVA
Winding 1 Voltage	400 kV
Winding 2 Voltage	150 kV
Winding 3 Voltage	34 kV
Leakage reactance (HL)	.23 pu
Leakage reactance (HT)	.23 pu (assumed)
Leakage reactance (LT)	.23 pu (assumed)
Copper loss	1600 kW

At the 150 kV buses, the load is assumed to have an active power and reactive power of 150 MW and 75 MVAr, respectively. One exception is made for the EEKLN150 kV bus, where the load is 75 MW and 37.5 MVAr. This leads to values for $\boldsymbol{R}$, $\boldsymbol{L}$ and $\boldsymbol{C}$ according to Table A.5.

Table A.4: Transformer B parameters

Nominal Power	600 MVA
Winding 1 Voltage	400 kV
Winding 2 Voltage	225 kV
Winding 3 Voltage	34 kV
Leakage reactance (HL)	.15 pu
Leakage reactance (HT)	.15 pu (assumed)
Leakage reactance (LT)	.15 pu (assumed)
Copper loss	830 kW

Bus voltage	P (MW)	Q (MVAr)	R (Ω)	L (H)	C (μF)
220 kV	250	125	193.6	1.23	8.22
150 kV	150	75	150	0.95	10.61
150 kV (EEKLN150)	75	37.5	300	1.9	5.3

Table A.5: Loads

EnergyVille unites the Flemish research institutes KU Leuven, VITO, imec and UHasselt for research on sustainable energy and intelligent energy systems.

EnergyVille
Thor Park 8310
3600 Genk, Belgium

info@energyville.be
+32 (0)14 33 59 10